Structural Engineering of Amphiphilic Block Copolymer Nano-assemblies for Cancer Therapy

MS Thesis Report submitted towards the partial fulfillment of

BS-MS dual degree program

By

SHARAFUDHEEN PC

20131020

Under the guidance of

Prof. M. JAYAKANNAN

Chair

Department of Chemistry

Indian Institute of Science Education and Research (IISER) Pune

March 2018

CERTIFICATE

This is to certify that this dissertation entitled "**Structural Engineering of Amphiphilic Block Copolymer Nano-assemblies for Cancer Therapy** " towards the partial fulfilment of the BS-MS dual degree programme at the Indian Institute of Science Education and Research, Pune represents work carried out by "**SHARAFUDHEEN PC** at IISER Pune" under the supervision of "Prof. M. Jayakannan, Professor, Chair, Department of chemistry" during the academic year 2017-2018.

Date: 20/03/2018
Place: Pune

Signature of student

Date: 20/03/2018
Place: Pune

Signature of Supervisor

DECLARATION

I hereby declare that the matter embodied in the report entitled "**Structural Engineering of Amphiphilic Block Copolymer Nano-assemblies for Cancer Therapy**" are the results of the work carried out by me at the Department of Chemistry, IISER Pune, under the supervision of Prof. M. Jayakannan and the same has not been submitted elsewhere for any other degree.

Date: 20/03/2018
Place: Pune

Signature of student

Date: 20/03/2018
Place: Pune

Signature of Supervisor

ACKNOWLEDGEMENTS

I am pleased to express my sincere gratitude towards my thesis supervisor **Prof. M. Jayakannan** for his prodigious guidance and constant encouragement and support throughout the project.

I am grateful to Dr. Sandanaraj Britto for being my TAC member and for his valuable suggestions in the TAC meetings.

I would like to thank Dr. Bapurao Surnar and Mehak Malhotra for their continuous aid and helps to overcome the hurdles in my way.

I am also grateful to all chemistry department faculties and for their support in pursuing my dreams at IISER.

I am indebted to all technical staff members Mahesh, Sandeep, Swati, Nitin, Ganesh for making my research easier at IISER.

Nothing would have been possible without my lab members. Special thanks to my present and past lab members Nilesh, Dr. Anantharaj, Dr. Rajendra, Dr. Narasimha, Bhagyashree, Ruma, Sonashree, Dheeraj, Sakshi, Anu, Abhishek, Uttareshvar, Pranav, Khuddus, Sharada, Yogita, Rasika, Mishika.

I am delighted to thank my parents, brother Suhail and sister Sajla for their love and support.

--Sharafu

Contents

List of figures and tables

Abstract

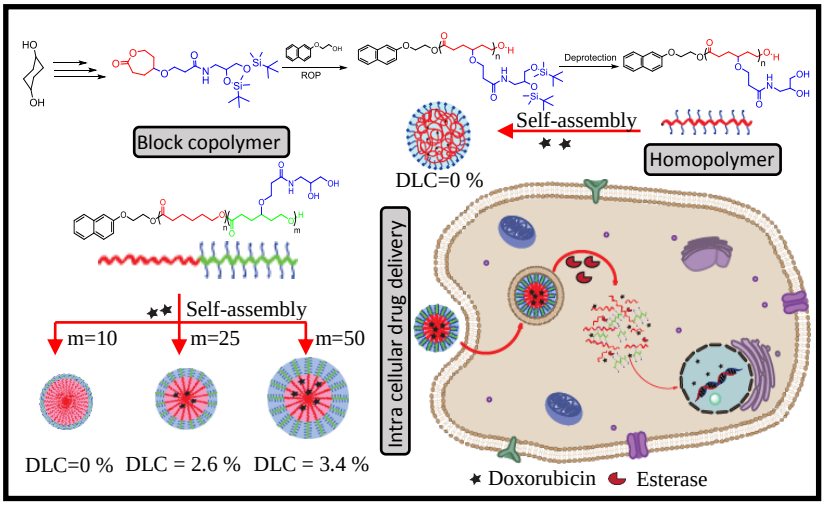

This thesis is aimed to design and develop amphiphilic polycaprolactone (PCL) block copolymer nanoscaffolds for intracellular drug delivery in cancer therapy. The amphiphilicity in the PCL block copolymer was accomplished through bis-hydroxyl substitution in the periphery of PCL backbone. For this purpose, a new γ-substituted caprolactone monomer containing silyl protected hydroxyl groups was tailor-made by multistep synthesis. The monomer underwent ring opening polymerization (ROP) by a newly designed naphthol based initiator to yield homopolymers and block copolymers. Silyl groups were de-protected to yield hydroxyl functionalized homo and block copolymers. Monomer and polymers were characterized using ^{1}H NMR, ^{13}C NMR, FTIR and HRMS and the molecular weights of the polymers were determined by gel permeation chromatography (GPC). Thermogravimetric analysis showed that the polymers were thermally stable up to 240 ^{o}C. Differential scanning calorimetry and polarized light microscope (PLM) techniques were used to study the semi-crystalline and amorphous natures of the polymers. Water contact angle (WCA) of the silyl-polymers were found be in the range of 90-100° with respect to hydrophobic nature. Whereas, the hydroxyl polymers were found to have WCA< 50° with respect to hydrophilic nature. These block copolymers self-assembled in water to produce micellar nanoparticles of <200 nm size. These nanoparticles were capable of encapsulating anticancer drugs like doxorubicin with excellent drug loading capabilities. These drugs loaded nanoparticles were characterized by dynamic light scattering (DLS) and electron microscopy. Enzymatic degradation of the polymers was studied using Dynamic light scattering (DLS). Confocal and flow cytometry analysis confirmed the cellular uptake of the doxorubicin loaded polymer nanoparticles in cancer cells.

1. Introduction

1.1. Block copolymers

Block copolymers are a class of copolymers in which different monomer units are arranged in blocks along the polymer chain. Advancements in polymerization techniques allowed for the synthesis of different block copolymer architectures like star, miktoarm star, comb, centipede, barbwire and comb star block copolymers with the combination of different controlled polymerization techniques and post polymerization modifications[1] (Figure 1.1).

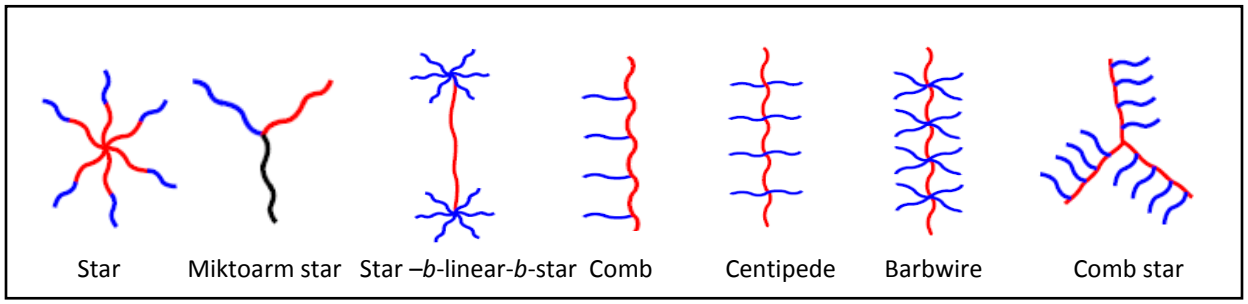

Figure 1.1: Different block copolymer architectures[1]

Block copolymers can be synthesized by various methods which can be broadly classified in to two. One with the sequential addition of monomers via controlled polymerization techniques like Atom radical polymerization (ATRP), Nitroxide mediated polymerization (NMP), Ring opening polymerization (ROP) etc. and the other via coupling of different blocks[2]. Lewis et al. published synthesis of a thermo-responsive ABA triblock copolymer using ATRP[3] (scheme 1.1 a). Nitroxide mediated polymerization (NMP) is another controlled polymerization technique which is typically used to synthesize poly vinyl acetates, poly dimethyl acrylamides etc. They may produce polymers with low molecular

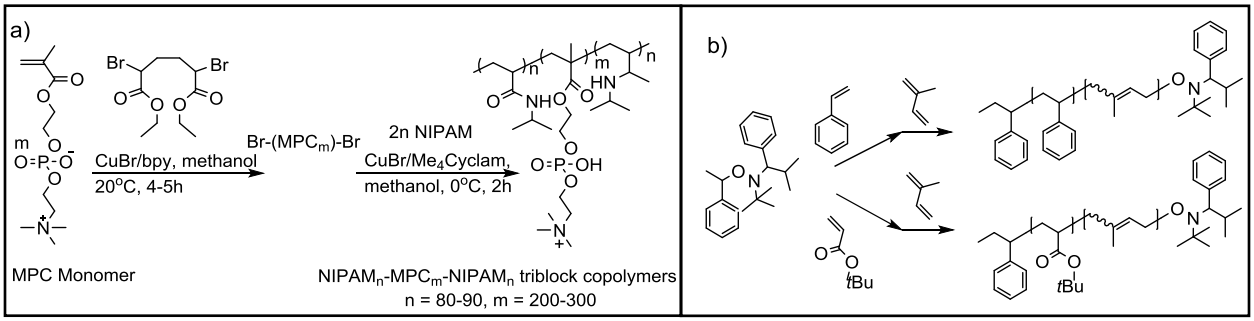

Scheme 1.1: a) Synthesis of triblock copolymer NIPAM-MPC-NIPAM using ATRP[3]. b) Synthetic scheme for block copolymers using modified NMP initiator[4].

weights and broad molecular weight distributions, but modifications have been made on the NMP initiators to overcome these limitations. Hawker et al. reported a modified NMP initiator for the polymerization of dienes to give narrow disperse polymers with high molecular weights[4] (scheme 1.1 b)

1.2. **Self-assembly of block copolymers**

Block copolymers can have hydrophilic and hydrophobic blocks, which makes some polymers hydrophobic, while others hydrophilic. The presence of both hydrophilic and hydrophobic blocks makes them amphiphilic. Amphiphilic polymers in water self-assemble to form nanoparticles with hydrophilic parts in contact with water. The nano particles formed can have different morphologies depending on the polymer composition. They can be spherical micelles, rods, lamallea, vesicles or bilayers[1,5]. These morphologies are primarily determined by a parameter named packing parameter (p=v/al, v = volume of the hydrophobic part, a = area of the hydrophilic head and l = length of the hydrophobic tail) (figure 1.2). Spherical micelles are formed when p≤1/3, cylindrical micelles have packing parameter 1/3≤p≤1/2, polymersomes like vesicles have ½≤p≤1.[1]

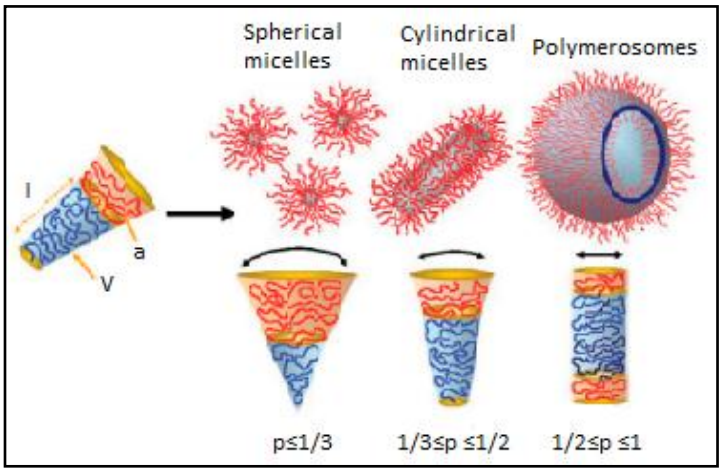

Figure 1.2: Parameters for the formation different nanocarriers[1]

Spherical micelles contain a spherical hydrophobic core and hydrophilic chains surrounding it. The hydrophilic coronas help in water solubility while the hydrophobic core can be used to load hydrophobic cargoes like drugs or fluorescent probes, hence it can be used as drug delivery vehicles as well as bioimaging agents. Cylindrical rods are similar to micelles, they are composed of hydrophobic core in cylindrical shape and a hydrophilic corona[5]. Vesicles have an architecture similar to cells, having a hydrophobic wall and hydrophilic coronas inside and outside. Having both

hydrophobic and hydrophilic pockets, they can be used to load both hydrophilic and hydrophobic drugs, hence can be used for combination therapy[5].

1.3. **Block copolymers in drug delivery**

Block copolymers having a well defined hydrophobic and hydrophilic part and with narrow dispersity will self-assemble to form nanocarriers with narrow size range. Self-assembly and drug loading in amphiphilic block copolymers can be done using various methods including dialysis method, oil in water (O/W) emulsion method, sonication method etc. The simplest method is the direct dissolution of polymer and the drug in water and loading is obtained by either heating on sonication. When the polymer is not completely soluble in water, a water miscible organic solvent is used to solubilize the polymer and is removed by dialysis or a water immiscible organic solvent is used and then removed by evaporation as done in O/W emulsion method. Various methods are briefly shown in figure 1.3.[2]

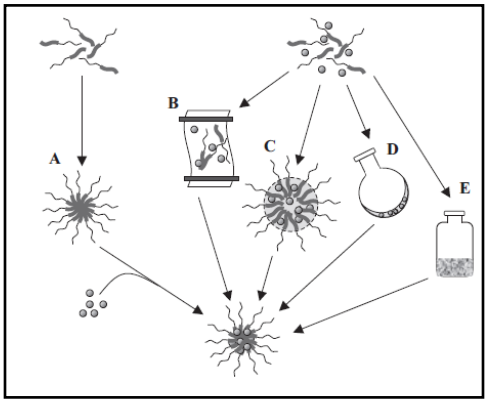

Figure 1.3: Different drug loading methods[2]

The drug loaded nanoparticles entering the blood stream will get selectively accumulated in cancer tissues owing to their leaky vasculature and lack of lymphatic drainage, a phenomenon known as Enhanced permeability and retention effect (EPR effect).[6] Once entered in the cancer tissue, nanocarriers will be taken up by endosomal pathways. Tagging targeting ligands like biotin on to the nanocarriers can enhance the selectivity towards the cancer cells owing to their over expression of receptors[7]. The cargoes inside the carrier vehicles will be released based on the stimuli present in the polymer. Some of them can be pH responsive, while others responsive to enzymes like esterase or chymotrypsin, they can have controlled or burst release[8].

1.4. **Biodegradable block copolymers**

Biodegradability is a desired property of polymers for biological applications. Several biodegradable polymers are approved by FDA for biomedical applications including Poly lactic acid (PLA), poly caprolactones (PCL), poly (lactic-co-glycolic acid) (PLGA), Amino acid based polymers, Poly hydroxy butyrate (PHB) (Figure 1.4). PLA are made from chiral

lactide monomers, which can be semi crystalline when the monomers are enantiomerically pure or amorphous when racemic. Esterase enzyme can cleave the ester bonds in PLA, which give natural metabolic byproduct lactic acid. PLGA is obtained by ring opening copolymerization of two monomers, the cyclic dimers of glycolic acid and lactic acid, which can be made in a random or block fashion. As in the case of PLA, PLGA also undergoes hydrolysis by esterase enzyme to glycolic acid and lactic acid. Polycaprolactones are synthesized by ring opening polymerization of cyclic lactones, which will be further discussed in the coming sessions.[9,10]

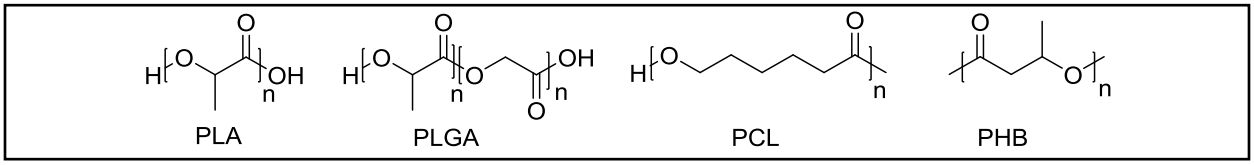

Figure1. 4: Different types of polyesters[9,10]

1.5. **Ring opening polymerization (ROP)**

Polyesters have been synthesized using step growth polymerization of diacids or diesters with diols, but the removal of byproducts methanol or water requires higher temperature or tedious procedures, limiting its molecular weight and dispersity properties, this paved the way for the development of a new procedure for making polyesters, Ring Opening Polymerization (ROP). ROP being a living polymerization technique overcomes the limitations of other polymerization methods, it gives rise to narrow molecular weight distribution of polymers, it has a good control over molecular weights and can be used to design block copolymers using different monomers. Different types of biodegradable and biocompatible polymers are synthesized using ROP. Polycaprolactones, poly valerolatones, Poly lactides and poly glycolides are some of them.[11,12,13] (Figure 1.5)

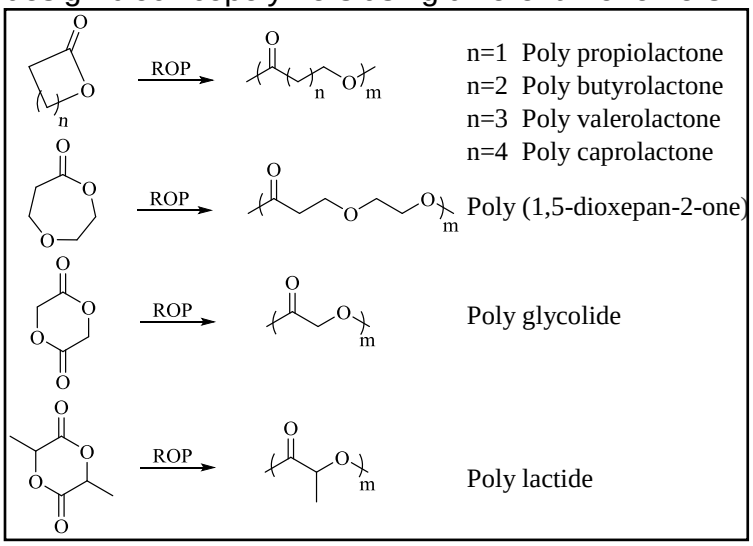

Figure 1.5: Different monomers for ROP and their polymers obtained by ROP[11]

Depending on the catalysts and initiators used in ROP, they have four different mechanisms, cationic, anionic, monomer activated and coordination insertion mechanisms. (figure 1.6). A wide variety of anionic, cationic and coordinative initiators or catalysts are available for ROP. In anionic ROP, an anionic initiator opens the ring at the carbonyl position of the monomer and hence produces an alkoxide as the growing species, which propagates further by opening more monomers. Cationic ROP propagates through nucleophilic substitution reaction in which a cationic species is initially attacked by the carbonyl oxygen in the monomer leaving behind a positive charge at the carbonyl carbon. In monomer activated ROP, the monomer is first activated by a catalyst and then opened by a suitable initiator. Many metal based catalysts are known for coordination insertion mechanism like tin octanoate, Scandium triflate, Aluminum isopropoxide, zinc alkoxides etc., in which the propagation proceeds through the coordination of the monomer and initiator to the catalyst by forming a metal oxygen bond. During the entire propagation process metal is attached to the growing chain through an alkoxide bond.[14]

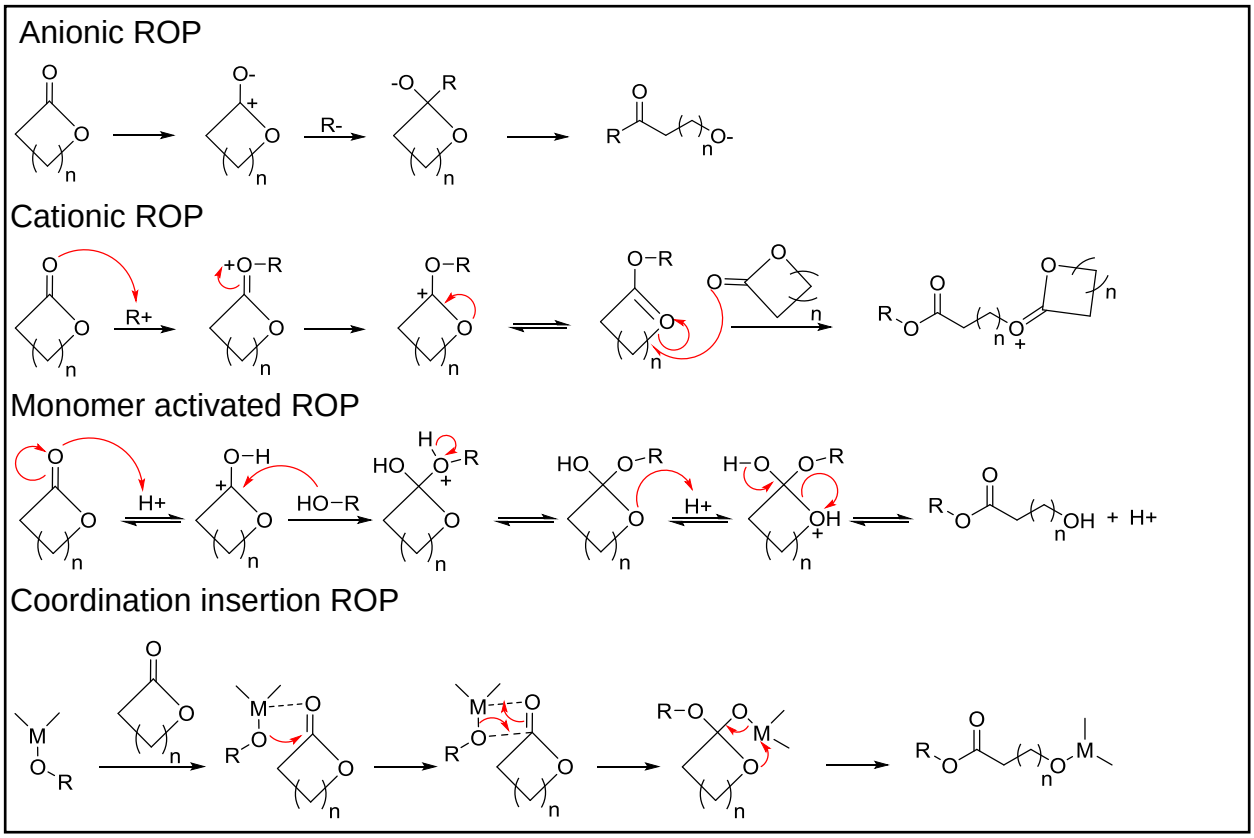

Figure 1.6: Different mechanisms of ROP

1.6. **Polycaprolactones**

Polycaprolactones (PCL) are a widely used polymer in biomaterials and drug delivery systems because of its biodegradability and biocompatibility. It's unique mechanical properties includes crystallinity, tensile properties like young's modulus, melting and decomposition temperatures, miscibility in various polymers like Poly vinyl chloride and poly styrene acrylonitrile. PCL can by synthesized either by condensation polymerization of 6-hydroxy hexanoic acid, Ring opening polymerization of ε caprolactone using variety of anionic, cationic, coordination catalysts (Scheme 1.2) or by Ring opening free radical polymerization of 2-methylene-1-3-dioxepane. The monomer for ROP ε caprolactone is synthesized from cyclohexanone by Baeyer Villiger oxidation as shown in scheme 1.2. ROP of ε caprolactone follows the mechanisms which are explained in the previous section, i.e. anionic, cationic, monomer initiated and coordination insertion mechanisms. There are lot of catalysts known for ROP, Alkali metal based catalysts are ionic compounds, they follows anionic mechanism, for example Lithium diisopropylamide (LDA). Magnesium and calcium containing catalysts are the most commonly used alkali earth metals because of their high activity, low toxicity and presence in biological systems. There are lot of aluminium based catalysts known, such as Triethyl aluminium, Aluminium triflates and Aluminium alkoxides. Stannous ethylhaxanoate is the most commonly used tin based catalyst.[14]

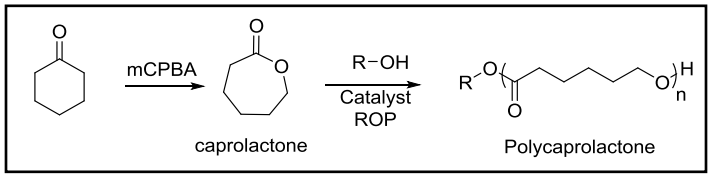

Scheme 1.2: Synthesis of caprolactone monomer and polycaprolactone polymer by ROP.

PCL has wide range of applications in medical devices like sutures, wound dressings, contraceptive devices, drug delivery vehicles, tissue engineering etc. PCL is used mostly in long term drug delivery systems because of its slow biodegradation. Its unique ability to form compatible blends with other polymers, makes efficient drug delivery systems with controlled release kinetics. PCL based micelles, vesicles and other nano forms can load both hydrophilic and hydrophobic drugs[15].

PCL being hydrophobic, it is also used to bring amphiphilicity to hydrophilic polymers to help it self-assemble in water and can be used for drug delivery and other biomedical purposes. Zifu Li et al reported a galactose functionalized hydroxyethyl starch grafted polycaprolactone nanoparticles (Gal-HES-PCL) were PCL acted as the hydrophobic core helping in the loading of hydrophobic anti-cancer drug Doxorubicin and photosensitizer indocyanine green (ICG) used for Photothermal therapy (PTT) as well as bio imaging[16].

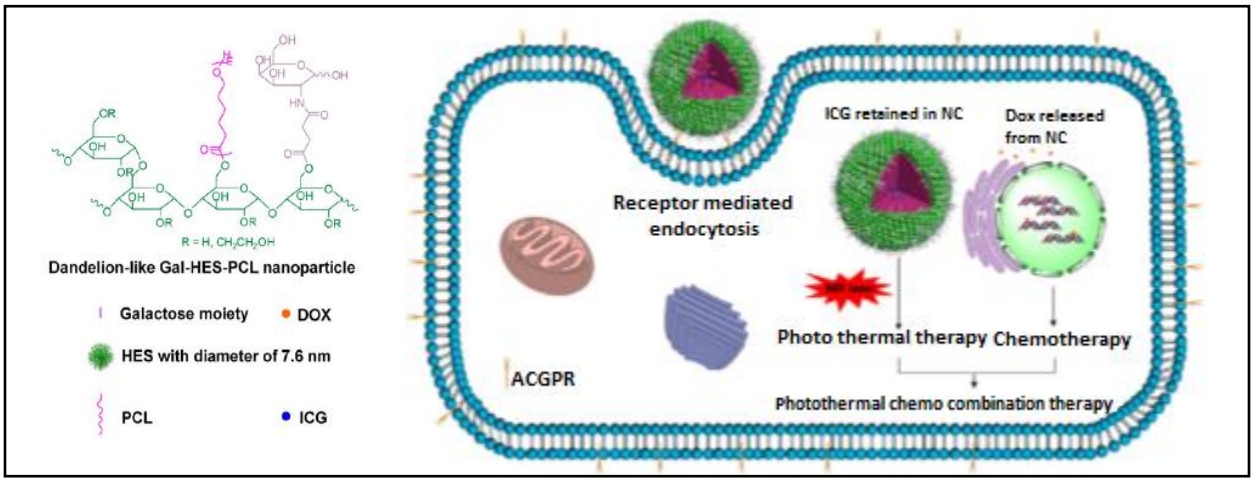

Figure 1.7: Structure of Gal-HES-PCL polymer and their use in Photothermal/Chemo combination therapy[16]

1.7. **Substituted caprolactones**

The hydrophobicity and crystallinity of PCL limits its applications in biomedical fields,

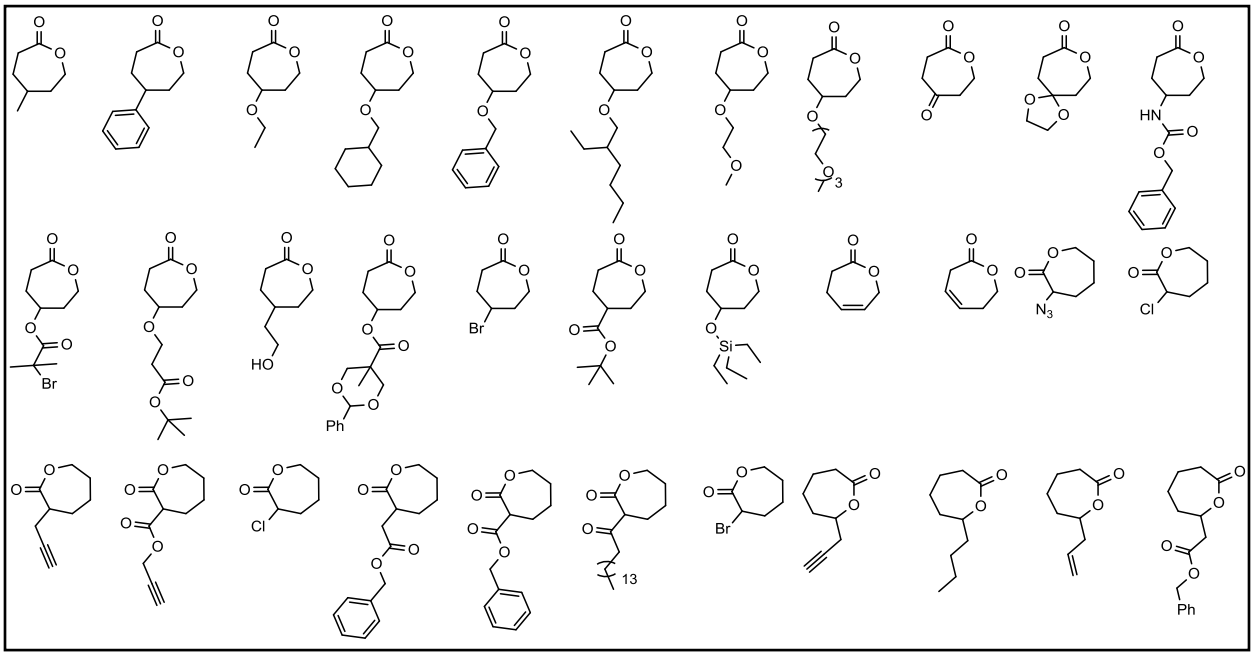

Figure 1.8: Different types of substituted caprolactone monomers[17,18]

which paved the way for the synthesis of substituted caprolactone monomers. This gave rise to many functional PCL and non-functional PCL with varying crystallinity, control over biodegradation, enhanced biocompatibility etc. Functional PCL also gives opportunities to conjugate drug molecules and targeting ligands[17,18].

Halogen functionalized PCL are used as macroinitiators for Atom transfer radical polymerization (ATRP), Zhang et al reported the synthesis of poly(ε-caprolactone)-graft-polystyrene by ATRP using poly(ε-caprolactone-co-α-bromo-ε-caprolactone) copolymer as the macroinitiator. Initially the macroinitiator P(CL-co-α-BrCL) was synthesized by ROP of εCL and α-bromo ε caprolactone which was then used as the macroinitiator for the synthesis of PCL graft polystyrene.[19]

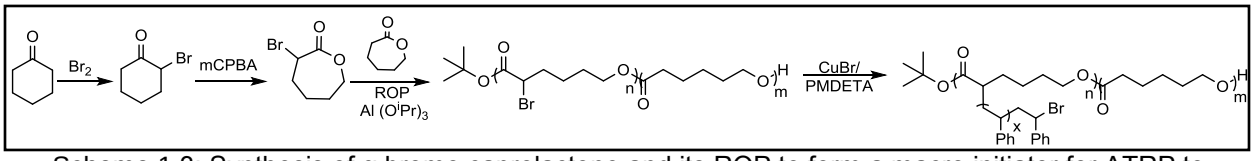

Scheme 1.3: Synthesis of α bromo caprolactone and its ROP to form a macro initiator for ATRP to synthesize PCL graft Polystyrene[19]

Lang et al reported the synthesis of γ amino substituted PCL giving pH responsiveness to the polymer. A new caprolactone monomer γ-(carbamic acid benzyl ester)-ε-caprolactone (γ CAB ε CL) was designed and subjected to ROP by polyethelene glycol monomethyl ether (mPEG), the amine protecting group was then hydrolyzed under acidic conditions. In basic or neutral pH these polymers self-assembled. Once the amine groups on PCL block got protonated in acidic pH, the amphiphilicity got disturbed and hence the self-assembly collapsed. Cancer tissues being acidic in nature, this is a potential candidate for the delivery of anticancer drugs.[20]

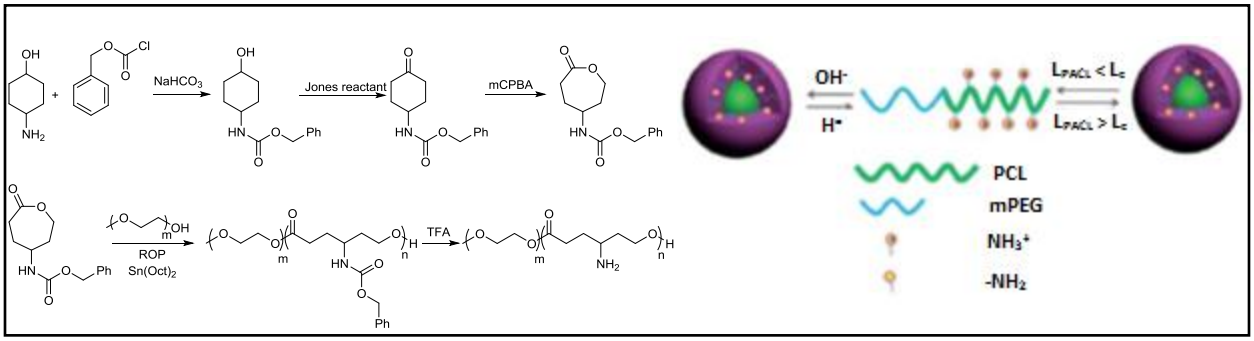

Figure 1.9: Synthesis of γ amino substituted PCL and the schematic illustration of pH and block length induced self-assembly of mPEG-*b*-PACL[20]

Bapu et al designed a carboxyl functionalized caprolactone monomer which has been used for wide range of applications. Initially a pH responsive vesicle was designed for dual drug delivery under gastro intestinal tract. Tertiary butyl protected carboxyl containing caprolactone monomer was designed from commercially available 1,4-cyclohexanediol and tertiary butyl acrylate, which was subjected to ROP by mPEG in the presence of $Sn(Oct)_2$ catalyst. Upon deprotection with Trifluoroacetic acid, carboxyl functionalized PCL polymers were obtained, which when self-assembled in water formed vesicles able to load both hydrophobic and hydrophilic anticancer drugs.

Carboxylic acid groups on the PCL chains were also used to stitch Cisplatin, an important anti-cancer drug. Cisplatin was chemically conjugated on to the carboxylic acid group on the polymer chains, which when self-assembled in water formed core shell nanoparticles. Cisplatin formed the core and PCL formed a layer protecting it from GSH detoxification[22]. Later, a triple block copolymer of mPEG, PCL and Carboxylic PCL (CPCL) was synthesized, cisplatin was conjugated on the CPCL block and then self-assembled to form a nanocarrier which loaded the anticancer drug Doxorubicin. Hence a new triple block nanocarrier was designed for synergistic combination therapy of antagonistic drugs cisplatin and doxorubicin for enhanced efficacy in cisplatin resistant breast cancer [23].

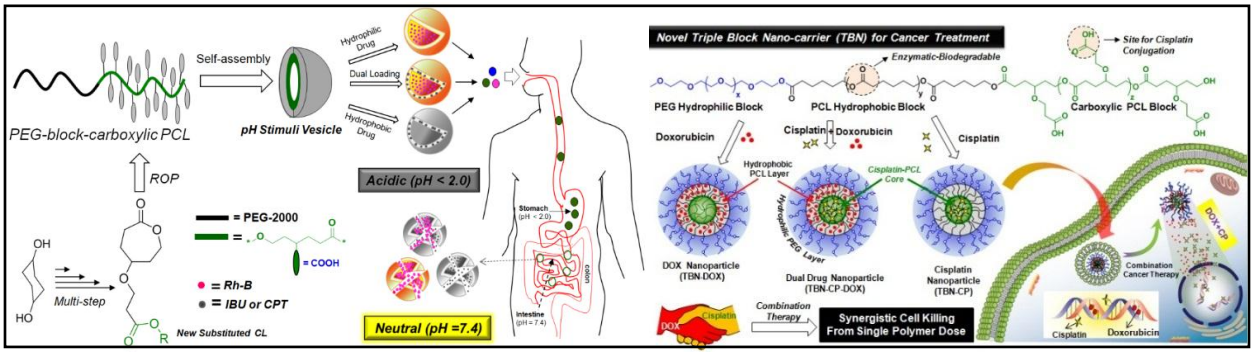

Figure 1.10: pH responsive delivery of anti-cancer drugs in the carboxylic PCL block copolymer vesicles under the GI tract[21], Synergistic combination therapy of cisplatin and doxorubicin using a triple block nanocarrier. [23]

Trollsas et al. reported the synthesis of two novel hydroxyl and bis hydroxyl containing polycaprolactones (Scheme 1.4). These two protected hydroxyl containing caprolactone monomers were designed from 1,4-cyclohexane diol, which was subjected to ROP in the presence of $Sn(Oct)_2$, and then the protecting groups were removed to form hydroxyl containing PCL[24].

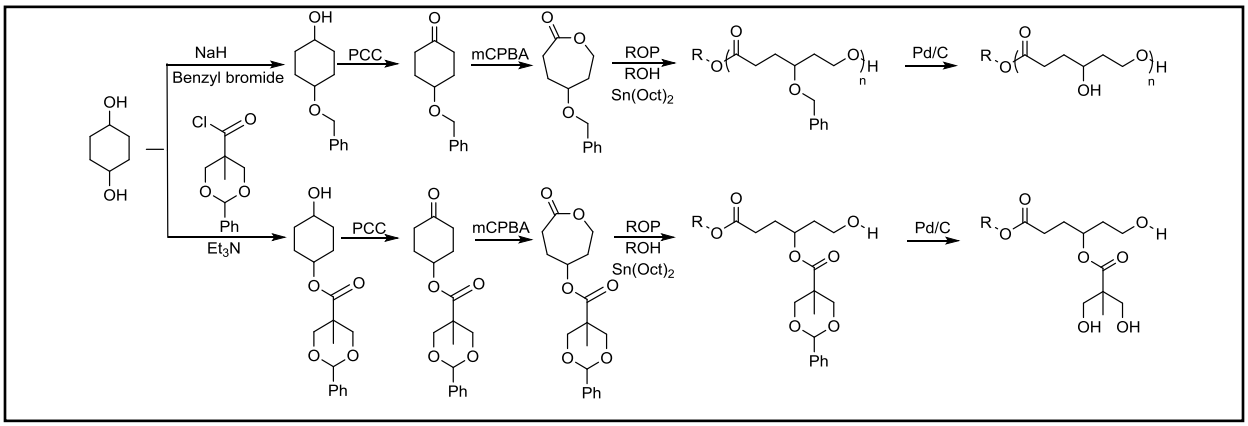

Scheme 1.4: Synthesis of mono and bis hydroxyl containing PCL[24]

Chang et al. reported a novel amphiphilic diblock copolymer with mPEG, PCL and PCL bearing pedant hydroxyl groups, which was used for doxorubicin delivery to cancer cells. A diblock was prepared by the ROP of CL and Substituted caprolactone TUSUO by mPEG. The acetal groups were deprotected to give ketones which were reduced to hydroxyls by sodium borohydride. Hydroxyl groups are biologically relevant functional groups present abundantly in biological systems. They can be used to conjugate drugs or dye molecules. Hydroxyls are known to form extensive hydrogen bonding, stabilizes Doxorubicin, increasing the loading efficiency of the nanocarrier and controlling the release kinetics[25].

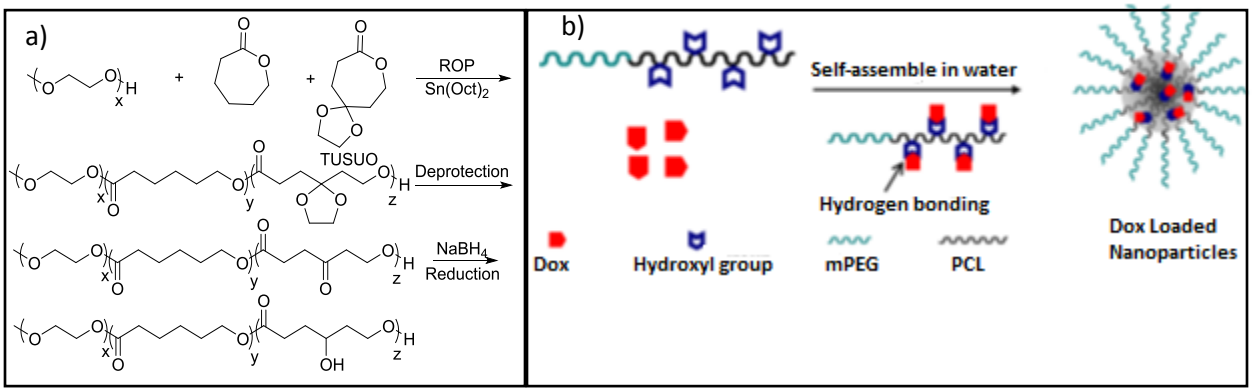

Figure 1.11: a) ROP of caprolactone monomers and post polymerization modifications to form hydroxyl pendant groups. b) Self-assembly and doxorubicin loading of the block copolymer[25]

1.8. **Non-PEGylated Polycaprolactones for drug delivery**

Poly ethylene glycols (PEG) are extensively used to ring open caprolactones because of its biocompatibility and hydrophilicity [27]. Absence of functional groups on PEG minimized the possibility of conjugating targeting ligands or drug molecules to the polymer chain.

When PEG-PCL self assembles, PEG being the corona of the nanocarrier, limits the option of tagging targeting ligands. Moreover PEG is not completely biodegradable.

There are very few reports for non-PEGylated PCL systems for drug delivery applications. Jing Hao et al. reported the synthesis of two caprolactone monomers γ-octyloxy-ε-caprolactone and γ-2-[2-(2-methoxyethoxy)ethoxy]ethoxy-γ-caprolactone and their ring opening polymerization with benzyl alcohol to form block copolymers. The self-assembly of these amphiphilic block copolymers were studied and was found to form micelles[26]. Rainbolt et al. from the same group used the same monomer to make diblock copolymers which were found to be thermo responsive and self-assembled to form micelles and loaded doxorubicin[28]. But in these reports the polymer does not have any functional groups present to conjugate any targeting ligands.

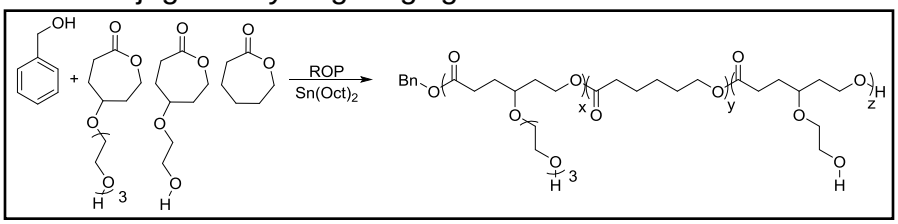

Scheme 5: ROP of monomer γ-2-[2-(2-methoxyethoxy)ethoxy]ethoxy-γ-caprolactone, γ-2-methoxyethoxy-ε-caprolactone and ε-caprolactone by benzyl alcohol[28]

Mehak et al. reported another non-PEGylated PCL system by the ROP of carboxylic functionalized caprolactone monomers and ε-caprolactone to form random and block copolymers. These polymers self-assembled in to nanoparticles of size less than 200 nm. They were used to load doxorubicin and invitro studies revealed their stability under physiological conditions and got cleaved by lysosomal esterase enzymes in the intracellular compartments. After self-assembly of these polymers, the carboxylic acid groups were present on the periphery of the nanoparticle, which can be used to conjugate targeting ligands containing hydroxyl or amine groups[29].

This thesis is aimed at the design of a new substituted caprolactone monomer containing protected hydroxyl groups which when polymerized using ROP technique under melt route, will give rise to a completely hydrophobic polymer and upon deprotection of the hydroxyls make it hydrophilic. These hydrophilic polymers can be a substitution for PEG which is a classic hydrophilic polymer and can be used to synthesize block copolymers with PCL as the hydrophobic part, bringing the amphiphilicity.

2. **Experimental methods**:

2.1. **Materials**:

1,4-Cyclohexanediol, potassium tert-butoxide, tert-butyl acrylate, pyridinium chlorochromate (PCC), molecular sieves (4Å), Trifluoroacetic acid (TFA), tert-butylchlorodimethylsilane, imidazole, m-chloroperbenzoic acid (m-CPBA), 1-Ethyl-3-(3-dimethylaminopropyl)carbodiimide (EDC.HCl), N,N-Diisopropylethylamine (DIPEA), Hydroxybenzotriazole (HOBt), 3-chloropropane-1,2-diol, sodium azide, triphenyl phosphene, 2-naphthol, 2-bromo ethanol, tin(II) 2-ethylhexanoate ($Sn(oct)_2$), Caprolactone (CL), Tetra-n-butylammonium fluoride (TBAF), nile red, Doxorubicin.HCl and esterase were purchased from Sigma Aldrich. Na_2SO_4, $NaHCO_3$, $Na_2S_2O_3$, Na_2SO_4, HCl, potassium carbonate and potassium iodide were purchased locally.

Solvents: Acetonitrile, diethyl ether, Tetrahydrofuran (THF), methanol, petroleum ether, Dichloromethane (DCM).

Methods:

^1H NMR samples were recorded using Bruker 400 MHz spectrophotometer in $CDCl_3$ or CD_3OD solvent using TMS as the standard. Gel permeation chromatography (GPC) was carried out using Viscotek VE 1122 pump, Viscotek VE 3580 RI and 3210 UV-Vis detectors. Samples for GPC were prepared in THF solvent and the results were obtained after calibration using polystyrene standards. Thermal stability of monomers, initiators and polymers were determined using Perkin-Elmer thermal analyzer STA 6000 model at 10°C/min heating rate. TA Q20 differential scanning calorimeter (DSC) was used to analyze the thermal properties of the polymers. Perkin-Elmer Lambda 45 UV-Visible spectrophotometer was used for the absorption studies. SPEX Fluorolog HORIBA JOBIN VYON fluorescence spectrophotometer was used to record emission spectra using a 150 W Xe lamp as the source of excitation at room temperature. MALDI-TOF of the polymers were recorded using Applied Bio systems 4800 PLUS MALDI TOF/TOF Analyzer. The mass of the small molecules was determined using a HRMS-ESI-Q-time-of-flight LCMS (SynaptG2, Waters). Nano ZS-90 apparatus was used to perform Dynamic light scattering (DLS) using a 633 nm red laser (at 90^o angle) from Malvern Instruments. DIGIDROP instrument GBX model was used to capture images of water drops on the polymer surface and image J software was used to measure the water contact angles. Zeiss Ultra Plus

scanning electron microscope was utilized to capture FESEM images. Samples were prepared by drop casting on to silicon wafers and evaporating the water at room temperature. LSM710 microscope was used to capture confocal micrographs of the drug loaded polymers after incubation with MCF 7 cells.

2.2. **Synthesis**:

2.2.1. Multistep synthesis of γ-substituted caprolactone (SiCL):

a) Synthesis of **tert-butyl 3-((-4-hydroxycyclohexyl)oxy)propanoate** (**1**): 1,4 Cyclohexanediol (35g, 301.7 mmol) was dissolved in dry THF (450 ml) under inert conditions. A catalytic amount of potassium t-butoxide (1 g) was added to this. t-Butyl acrylate (40 g, 241.4 mmol) dissolved in dry THF (50 ml) was added dropwise at 25 ^{o}C using a dropping funnel and after the addition, reaction mixture was refluxed for 36 h. THF was evoporated using rotavapor, and the unreacted 1,4 Cyclohexanediol was reprecipitated using cold DCM. DCM was evaporated and the product was obtained as a pale coloured viscous liquid (**1**). Further purification was done by column chromatography using ethyl acetate and hexane (1:5 v/v). Yield = 33g (40%)

^{1}H NMR (400 MHz, $CDCl_3$) δ ppm: 3.65 (m, 3H, O−C**H**$_2$− and O−C**H**), 3.30−3.40 (m, 1H, C**H**−OH), 2.44 (t, 2H, −C**H**$_2$CO−), 1.97−1.82 (m, 4**H**, -C**H**$_2$-), 1.64−1.30 (m, 4H, -C**H**$_2$-), 1.42 (s, 9H, -C**H**$_3$). ^{13}C NMR (100 MHz, $CDCl_3$) δ ppm: 171.09, 80.42, 69.51, 63.95, 63.52, 32.53, 30.34, 29.18, and 27.43. FT-IR (cm^{-1}): 3422, 2978, 2934, 2862, 1726, 1455, 1392, 1365, 1254, 1153, 1105, and 1032. HR-MS (ESI+): m/z [M + Na^+] for $C_{13}H_{24}O_4$ = 267.1562.

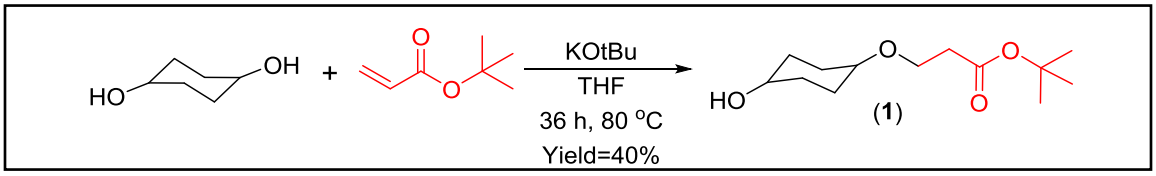

Scheme 2.1

b) Synthesis of **t-Butyl-3-((4-oxocyclohexyl)oxy)-propanoate** (**2**): compound **1** (30g, 122.9 mmol) was dissolved in dry DCM (400 ml) under inert atmosphere and stirred at 25°C. PCC (53g, 245.9 mmol) was added slowly along with molecular sieves (4 Å) and the reaction mixture was stirred for 6 h. The reaction mixture was filtered and washed

with DCM and further purified by passing over silica column using ethyl acetate and hexane (1:10 v/v) to obtain a colourless liquid product (**2**). Yield = 27g (95%)

^{1}H NMR (400 MHz, $CDCl_3$) δ ppm: 3.74 (m, 3H, O−C**H**$_2$- and O−C**H**-), 2.57 (m, 2H, −(CO)C**H**$_2$−), 2.49 (t, 2H, −C**H**$_2$−), 2.20 (m, 2H, −C**H**$_2$−), 2.08 (m, 2H, −C**H**$_2$−), 1.88 (m, 2H, −C**H**$_2$−), 1.42 (s, 9H, −C**H**$_3$). ^{13}C NMR (100 MHz, $CDCl_3$) δ ppm: 211.41, 170.98, 80.52, 72.73, 64.01, 37.01, 36.54, 30.41, 20.03. FT-IR (cm^{-1}): 2973, 2873, 2361, 1715, 1457, 1418, 1392, 1365, 1305, 1248, 1212, and 1101. HRMS (ESI+): m/z [M + Na^+] for $C_{13}H_{22}O_4$ = 265.1411.

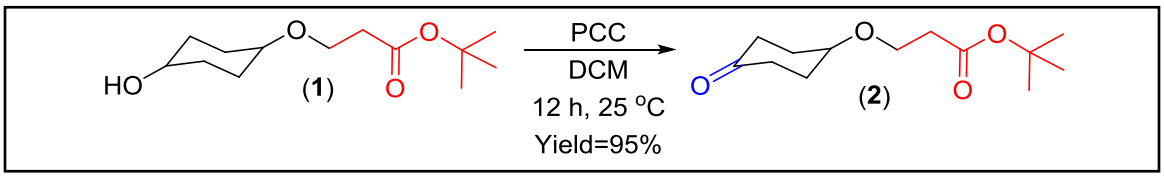

Scheme 2.2

c) Synthesis of **3-((4-oxocyclohexyl)oxy)propanoic acid** (**3**): Trifluoroactetic acid TFA (22 mL, 289 mmol) was added to a solution of compound **2** (10g, 41.3 mmol) in 25 mL DCM and the reaction mixture was stirred for 1 h at 25 °C. TFA and DCM were evaporated using rotavapor and the crude product was further purified by passing over silica column using ethyl acetate and petroleum ether (2:5 v/v) to obtain a light yellow liquid product (**3**). Yield = 7.3g (98%).

^{1}H NMR (400 MHz, $CDCl_3$) δ ppm: 9.46 (s, 1H, -COO**H**), 3.76 (t, 2H, -O-C**H**$_2$-), 3.74 (m, 1H, -O-C**H**-), 2.64 (s, 2H, -C**H**$_2$-), 2.56 (m, 2H, −C**H**$_2$−), 2.25 (m, 2H, -C**H**$_2$−), 2.06 (m, 2H, −C**H**$_2$−), 1.88 (m, 2H, -O-C**H**$_2$−). ^{13}C NMR (100 MHz, $CDCl_3$) δ ppm: 212.27, 177.12, 72.83, 63.28, 36.86, 36.04, and 30.22. FT-IR (cm^{-1}): 3445, 2930, 2361, 1701, 1419, 1345, 1305, 1244, 1188, 1104, and 1062. HRMS (ESI+): m/z [M + Na^+] for $C_9H_{14}O_4$=209.0784

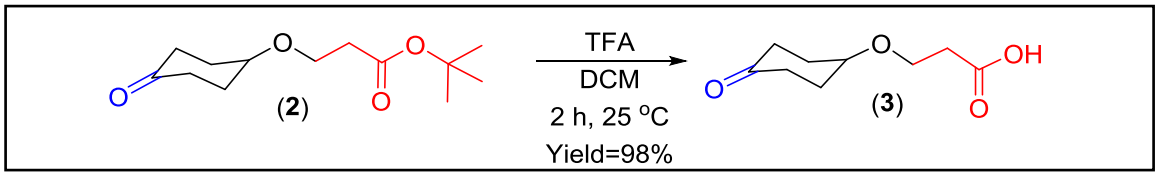

Scheme 2.3

d) Synthesis of **5-(chloromethyl)-2,2,3,3,8,8,9,9-octamethyl-4,7-dioxa-3,8-disiladecane** (**4**): Imidazole (25g, 360 mmol) was added in to a solution of 3-

chloropropane-1,2-diol (10g, 90 mmol) in 45 mL dry DMF and stirred under inert conditions. tert-butylchlorodimethylsilane (TBDMS Cl) (34g, 226 mmol) was added to the reaction mixture and was stirred for 12 h at 25 ^{o}C. DMF and unreacted TBDMS Cl (boiling point = 125 ^{o}C) were distilled completely and the residue was dissolved in DCM and washed with water. The organic layer was dried over anhydrous Na_2SO_4 and was concentrated using rotavapor and further purification was done by column chromatography using ethyl acetate and hexane (1:20 v/v) to obtain a colourless liquid product (**4**). Yield = 27g (96%).

^{1}H NMR (400 MHz, $CDCl_3$) δ ppm: 3.86 (m,1H, -O-C**H**-), 3.58 (m, 3H, -O-C**H**$_2$-, Cl- C**H**$_2$-), 3.48 (dd, 1H, Cl- C**H**$_2$-), 0.89 (s, 18H, -C-C**H**$_3$), 0.09(m, 12H, Si-CH_3). ^{13}C NMR (100 MHz, $CDCl_3$) δ ppm: 73.60, 65.14, 47.21,26.35, 26.23, 18.75,18.59, -4.10, -4.99. FT-IR (cm^{-1}): 2941.30, 2860.19, 1467.09,1359.81, 1253.20, 1122.32, 1080.92, 977.53, 942.25, 829.76, 773.06, 668.56, 572.80. HRMS (ESI+): m/z [M + H$^+$] for $C_{15}H_{35}ClO_2Si_2$ = 339.1354

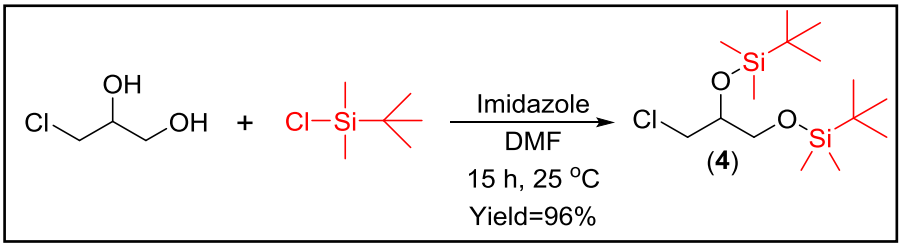

Scheme 2.4

e) Synthesis of **5-(azidomethyl)-2,2,3,3,8,8,9,9-octamethyl-4,7-dioxa-3,8-disiladecane** (**5**): Sodium azide (NaN_3, 19 g, 29 mmol) was added to the solution of compound **4** (33g, 97 mmol) in 200 mL dry DMF and then refluxed for 24 h. DMF was completely distilled out, the crude product was dissolved in ethyl acetate and washed with excess of water and then purified by passing over silica column using ethyl acetate and hexane (1:20 v/v) to obtain a colourless liquid product (**5**). Yield = 33.6g (90%).

^{1}H NMR (400 MHz, $CDCl_3$) δ ppm: 3.81 (m,1H, -O-C**H**-), 3.56 (m, 2H -O-C**H**$_2$-), 3.39 (dd, 1H, N_3-C**H**$_2$-), 3.18 (dd, 1H, N_3-C**H**$_2$-), 0.89 (s, 18H, -CH-C**H**$_3$), 0.09 (m, 12 H, Si-C**H**$_3$).

^{13}C NMR (100 MHz, $CDCl_3$) δ ppm: 72.66, 64.58, 54.37, 26.01, 25.89, 18.41, 18.17, -4.51, -5.33. FT-IR (cm^{-1}):2936.39, 2862.04, 2099.74, 1466.78, 1361.07, 1254.08, 1097.23, 987.37, 935.74, 830.70, 773.51, 728.25, 669.83, 561.51. HRMS (ESI+): m/z [M + H$^+$] for $C_{15}H_{35}N_3O_2Si_2$ = 346.2132

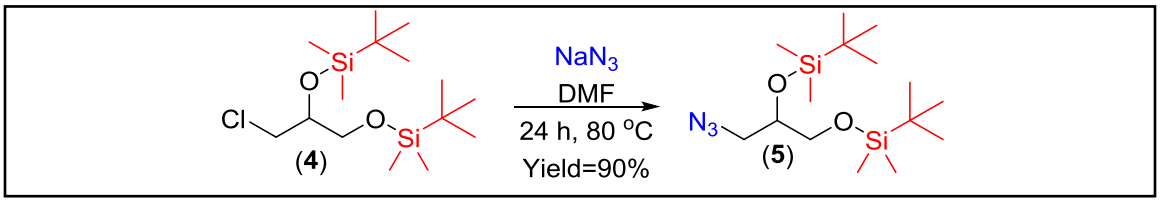

Scheme 2.5

f) Synthesis of **2,3-bis((tert-butyldimethylsilyl)oxy)propan-1-amine** (**6**): Triphenyl phosphene (PPh_3, 45.6g, 174 mmol) was added to compound **5** (30g, 86 mmol) in 150 mL THF and was stirred for 10 h under inert conditions. 20 mL water was added to it and then allowed to stir for 2 more hours. The solvent was completely evaporated and the crude product was dissolved in ethyl acetate and dried over anhydrous Na_2SO_4. The byproduct Triphenylphosphene oxide was separated by reprecipitation in diethylether. Diethyl ether was evaporated and further purification was done by column chromatography using ethyl acetate and hexane (3:10 v/v) to obtain a colourless liquid product (**6**). Yield = 28g (90%).

^{1}H NMR (400 MHz, $CDCl_3$) δ ppm: 3.61 (m,1H, -O-C**H**-), 3.53 (m, 2H -O-C**H**$_2$-), 2.8 (dd, 1H, H_2N -C**H**$_2$-), 2.7 (dd, 1H, H_2N -C**H**$_2$-), 0.89 (s, 18H, -CH-C**H**$_3$), 0.09(m, 12 1H-C**H**$_3$).

^{13}C NMR (100 MHz, $CDCl_3$) δ ppm: 74.62, 65.42, 45.82, 26.35, 26.29, 18.72, 18.55, -3.96, -5.00. FT-IR (cm^{-1}): 2937.86, 2859.39, 1466.79, 1363.18, 1252.56, 1078.12, 1001.93, 935.44, 829.90, 771.68, 667.79, 609.12, 570.09, 530.32. HRMS (ESI+): m/z [M + H^+] for $C_{15}H_{37}NO_2Si_2$ = 320.2442

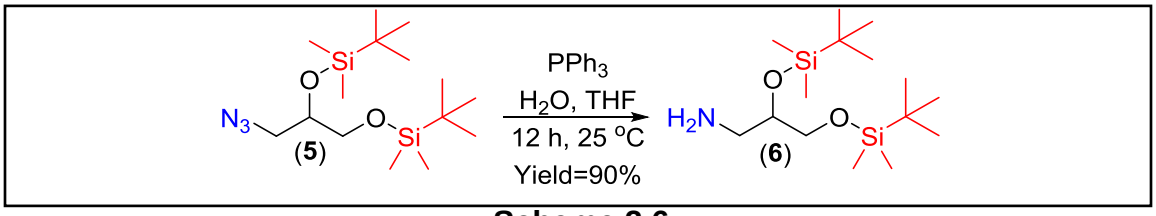

Scheme 2.6

g) Synthesis of **N-(2,3-bis((tert-butyldimethylsilyl)oxy)propyl)-3-((4-oxocyclohexyl)oxy)propanamide** (**7**): HOBt (4.35g, 32 mmol) and DIPEA (17 mL, 96 mmol) was added to a solution of compound **3** (6g, 32 mmol) and EDC.HCl (9.25g, 48 mmol) in 45 mL DCM under nitrogen purging and the reaction mixture was stirred for 30 minutes at 25 °C . Compound **6** (14.4g, 45 mmol) was added to the reaction mixture under nitrogen purging and the reaction mixture was stirred for 24 h at 25 °C. The reaction

mixture was washed with water. The organic layer was dried over anhydrous Na_2SO_4 and was concentrated using rotavapor, further purification was done by column chromatography using ethyl acetate and hexane (2:5 v/v) to obtain a colourless liquid product (**7**). Yield = 11g (60%).

^{1}H NMR (400 MHz, $CDCl_3$) δ ppm: 6.2 (s, 1H, -(CO)-N**H-**), 3.77 (m, 3H, -O-C**H-,** -C**H**$_2$-O-), 3.73 (m,1H, -O-C**H-**), 3.55 (m, 2H, -C**H**$_2$-NH-), 3.38 (t, 2H, -C**H**$_2$-O-), 2.53 (m, 2H, -C**H**$_2$-), 2.45 (t, 2H, -C**H**$_2$-), 2.26 (m, 2H, -C**H**$_2$−), 2.03 (m, 2H, −C**H**$_2$−), 1.94 (m, 2H, -C**H**$_2$-), 0.87 (s, 18H, -CH-C**H**$_3$), 0.05 (s, 12H, -Si-C**H**$_3$). ^{13}C NMR (100 MHz, $CDCl_3$) δ ppm: 211.40, 171.38, 73.70, 71.67, 66.18, 64.89, 43.29, 38.03, 37.59, 30.92, 26.35, 18.74, 18.53, -4.40, -4.99. FT-IR (cm^{-1}): 3312.22, 2937.24, 2860.49, 1714.82, 1655.59, 1543.18, 1465.63, 1360.68, 1251.20, 1096.91, 993.79, 830.91, 774.18, 668.83, 572.05

HRMS (ESI+): m/z [M + H^+] for $C_{23}H_{46}NO_5Si_2$ = 488.3233

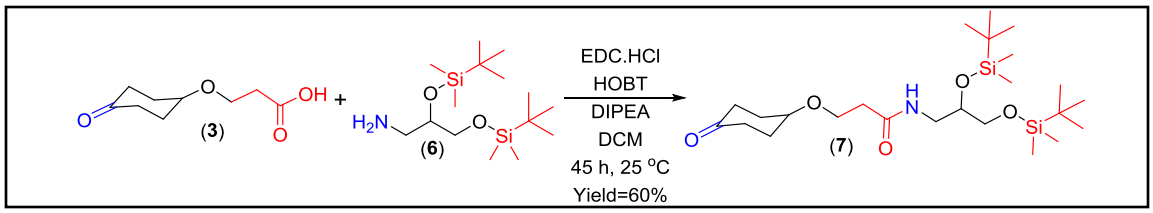

Scheme 2.7

h) Synthesis of **N-(2,3-bis((tert-butyldimethylsilyl)oxy)propyl)-3-((7-oxooxepan-4-yl)oxy)propanamide** (SiCL)(**8**): mCPBA (9.5g, 50 mmol) was added to a solution of compound **7** (9g, 18 mmol) in 200 mL dry DCM under nitrogen atmosphere. $NaHCO_3$ (4.7g, 50 mmol) was added in to the reaction mixture and then stirred at 25°C for 15 h. After the completion of the reaction (monitored by TLC), the reaction mixture was quenched with saturated aqueous solution of $NaHCO_3$ and $Na_2S_2O_3$, product was extracted to DCM and the organic layer was dried over anhyd. Na_2SO_4. DCM was evaporated completely and the crude product was purified by passing over silica column using ethyl acetate and hexane (2:5 v/v) to obtain a pale yellow coloured liquid product (**8**). Yield = 8g (80%)

^{1}H NMR (400 MHz, $CDCl_3$) δ ppm: 6.07(s, 1H, -N**H**-), 4.42 (m, 1H, -O-C**H**$_2$-), 4.01 (m, 1H, -O-C**H**$_2$-), 3.7 (m, 4H, -O-C**H**-, -O-C**H**$_2$-, -O-C**H**-), 3.55(m, 2H, -NH-C**H**-), 3.37 (m, 2H, -O-C**H**$_2$-), 2.92 (m, 1H, -O-C**H**$_2$-), 2.41 (m, 3H, -(CO)-C**H**$_2$-), 1.98 (m, 4H, -C**H**$_2$-), 0.87 (s, 18H, -CH-C**H**$_3$), 0.05 (s, 12H, -Si-C**H**$_3$). ^{13}C NMR (100 MHz, $CDCl_3$) δ ppm: 176.64, 171.33,

75.20, 71.87, 66.59, 64.99, 64.10, 43.73, 38.20, 34.60, 28.62, 28.13, 26.54, 19.04, 18.84, -3.78, -4.69. FT-IR (cm^{-1}): 2937.54, 2861.42, 1724.82, 1655.62, 1543.18, 1465.63, 1360.68, 1251.20, 1096.91, 993.79, 830.91, 774.18, 668.93, HRMS (ESI+): m/z [M + H^+] for $C_{23}H_{46}NO_5Si_2$ = 504.3183

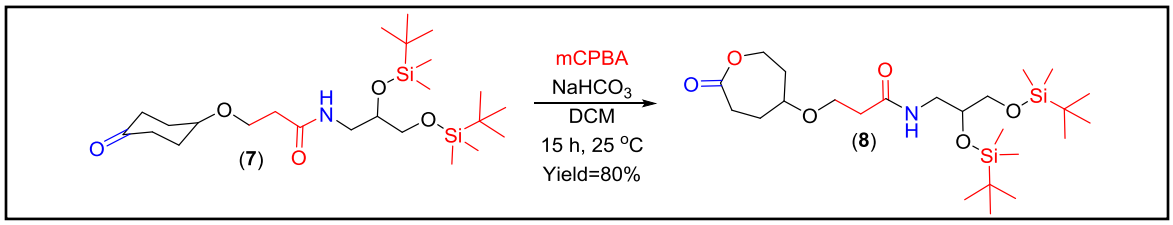

Scheme 2.8

2.2.2. Synthesis of **2-(naphthalen-2-yloxy)ethan-1-ol** (NAP-OH)(**9**): Potassium carbonate (7.2g, 52 mmol) was added into a solution of naphthalen-2-ol (3g, 20.8 mmol) in 30 mL dry DMF under inert conditions and stirred for 30 minutes. Bromoethanol (3.9g, 31.3 mmol) and a catalytic amount of KI was added to the reaction mixture and stirred for 48 h. The entire amount of DMF was distilled under reduced pressure and the residue was dissolved in water and product was extracted into ethyl acetate and the organic layer was dried over anhyd. Na_2SO_4. Ethyl acetate was evaporated and the crude product was further purified by passing over silica column using ethyl acetate and hexane (1:5 v/v) to obtain a light brown solid product (**9**). Yield = 2 g (51%)

1H NMR (400 MHz, $CDCl_3$) δ ppm: 7.77 (m, 3H, -C**H**-), 7.46 (m, 1H, -C**H**-), 7.35 (m, 1H, -C**H**-), 7.16 (m, 2H, -C**H**-), 4.21 (t, 2H, -O-C**H**$_2$-), 4.04 (m, 2H, HO-C**H**$_2$-), 2.08 (t, 1H,-O**H**).

13C NMR (100 MHz, CDCl3) δ ppm: 157.01, 134.92, 130.00, 129.59, 128.12, 127.23, 126.92, 124.27, 119.17, 107.31, 69.65, 61.98. FT-IR (cm^{-1}): 3337.68, 2982.90, 2860.58, 1588.27, 1447.80, 1206.95, 1042.48, 829.95, 734.54, 536.99

HRMS (ESI+): m/z [M + H^+] for $C_{12}H_{12}O_2$: 189.0843

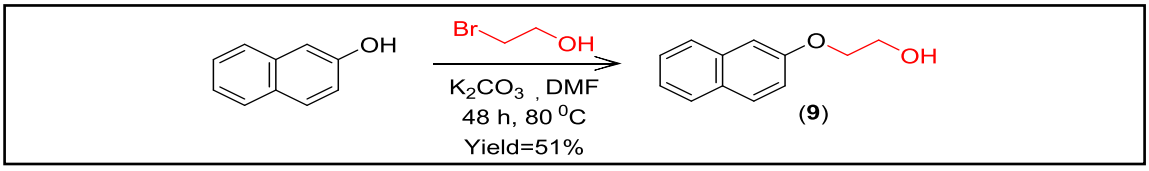

Scheme 2.9

2.2.3. Ring opening Polymerization (ROP) of caprolactones (CL):

a) Synthesis of PCL: The typical synthetic procedure is elucidated for PCL_{50}, where initial monomer to initiator ratio ($[M_0]/[I_0]$) was kept 50. The initiator NAP-OH (**9**) (16.49

mg, 0.087 mmol), catalyst $Sn(Oct)_2$ (17.77 mg, 0.044 mmol) and the caprolactone monomer (500 mg, 4.38 mmol) were taken in a flame dried Schlenk tube. High vacuum was applied to this reaction mixture for 45 min at room temperature. It was immersed in a preheated oil bath at 110 °C and stirred for 4 h. The Schlenk tube was cooled to room temperature and the polymer was dissolved in THF and precipitated in cold methanol. The precipitation in methanol was repeated at least twice to obtain pure polymer by dissolving in THF. Yield: 400 mg (75 %).

^{1}H -NMR (400 MHz, $CDCl_3$) δ ppm: 7.76 (m, 0.06H), 7.5(m,0.02H), 7.36(m, 0.02H), 7.16 (m, 0.04H), 4.48 (t, 0.04H), 4.3 (t, 0.004H), 4.07 (t, 2H), 2.3 (t, 2H), 1.62 (m,4H), 1.36 (m, 2H). FT-IR (cm^{-1}): 2940.30, 2862.73, 1719.72, 1364.60, 1237.74, 1173.01, 956.85, 727.66. GPC molecular weights: Mn = 5400g/mol , Mw = 6500 g/mol, and Mw/Mn = 1.2

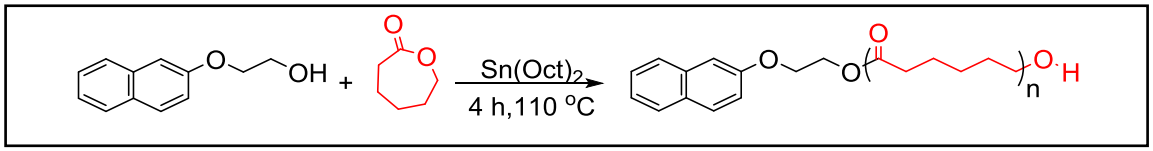

Scheme 2.10

b) Synthesis of SiPCL: The typical synthetic procedure is explained for $SiPCL_{10}$, were initial monomer to initiator ratio ($[M_0]/[I_0]$) was kept 10. The initiator NAP-OH (**9**) (18.66 mg, 0.099 mmol), catalyst $Sn(Oct)_2$ (20.1 mg, 0.049 mmol) and the SiCL (8) monomer (500 mg, 0.99 mmol) were taken in a flame dried Schlenk tube. High vacuum was applied to this reaction mixture for 45 min at room temperature. It was immersed in a preheated oil bath at 130 °C and stirred for 8 h. The Schlenk tube was cooled to room temperature and the polymer was dissolved in THF and precipitated in cold acetonitrile. The precipitation in acetonitrile was repeated at least twice to obtain pure polymer by dissolving in THF. Yield: 400 mg (75 %).

^{1}H -NMR (400 MHz, CH_3OD) δ ppm: 7.71 (m, 0.06 H), 7.43 (m, 0.02 H), 7.32 (m, 0.02 H), 7.14 (m, 0.04 H), 4.51 (t, 0.03 H), 4.32 (t, 0.03 H), 4.14 (t, 2 H) 3.85 (m, 1 H), 3.73 (m, 3 H), 3.57 (m, 2 H), 3.47 (m, 1 H), 3.25 (m, 1 H), 2.42 (m, 4 H), 1.78 (m, 4 H), 0.91 (s, 18 H), 0.08 (s, 12 H). FT-IR (cm^{-1}): 3305.81, 2936.57, 2859.96, 1731.12, 1651.06, 1251.70, 1093.88, 831.03, 773.34. GPC molecular weights: Mn= 3900g/mol, Mw = 4800g/mol, and Mw/Mn =1.2

Similarly other homopolymers $SiPCL_{50}$ and $SiPCL_{100}$ were synthesized.

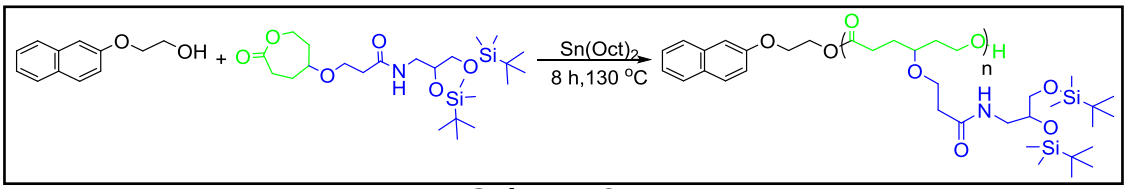

Scheme 2.11

c) Synthesis of $HyPCL_{50}$: $SiPCL_{50}$ (250 mg, 49 mmol) was dissolved in a mixture of 5 mL dry THF and 5 mL dry methanol, TBAF in 1 M THF (1.48 mL, 1.48 mmol) was then added drop wise at 0 °C and then the reaction mixture was stirred for 24 h at 25 °C, the reaction mixture was then quenched using 1N HCl. The entire amount of solvent was evaporated and the polymer was purified by dialysis.

^{1}H -NMR (400 MHz, CH_3OD) δ ppm: 7.76 (m, 0.06 H), 7.40 (m, 0.02 H), 7.33 (m, 0.02 H), 7.16 (m, 0.04 H), 4.51 (t, 0.03 H), 4.34 (t, 0.03 H), 4.16 (t, 2 H) 3.71 (m, 1 H), 3.70 (m, 3 H), 3.57 (m, 2 H), 3.47 (m, 1 H), 3.25 (m, 1 H), 2.45 (m, 4 H), 1.81 (m, 4 H). FT-IR (cm^{-1}): 3311.82, 2934.27, 2859.96, 1711.12, 1646.06, 1251.70, 1095.88, 831.03, 734.34

Other homopolymers $HyPCL_{50}$ and $HyPCL_{100}$ were obtained with the same synthetic protocol.

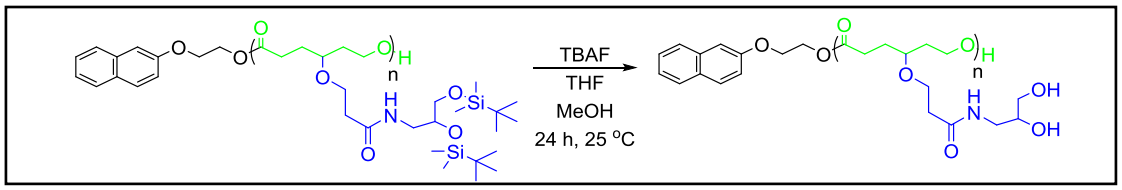

Scheme 2.12

2.2.4. Synthesis of block copolymers by ROP:

a) Synthesis of PCL-*b*-SiPCL: A typical synthetic procedure is elucidated for PCL_{50}-*b*-$SiPCL_{10}$, where initial monomer to macro initiator (PCL_{50}) ratio ($[M_0]/[I_0]$) is kept as 10. First the macro initiator PCL_{50} (468.4 mg, 0.079 mmol), catalyst $Sn(Oct)_2$ (16.08 mg, 0.039 mmol) and the caprolactone monomer SiCL (400 mg, 0.79mmol) were taken in a flame dried Schlenk tube. High vacuum was applied to this reaction mixture for 45 min at room temperature. It was immersed in a preheated oil bath at 130 °C and stirred for 8 h. The Schlenk tube was cooled to room temperature and the polymer was dissolved in THF and precipitated in cold methanol. The precipitation in methanol was repeated at least twice to obtain pure polymer by dissolving in THF.

^{1}H -NMR (400 MHz, $CDCl_3$) δ ppm: 7.75 (m, 0.06 H), 7.44 (m, 0.02 H), 7.36 (m, 0.02 H), 7.15 (m, 0.04 H), 6.20 (s, 1 H), 4.49 (t, 0.03 H), 4.30 (t, 0.03 H), 4.13 (t, 2 H), 4.07 (t, 2H), 3.80 (m, 1 H), 3.70 (m, 2 H), 3.54 (m, 2 H), 3.39 (m, 3 H), 2.40 (m, 4 H), 2.3 (t, 2H), 1.78 (m, 4 H), 1.62 (m,4H), 1.36 (m, 2H), 0.90 (s, 18 H), 0.09 (s, 12 H). FT-IR (cm^{-1}): 3309.84, 2938.47, 2861.26, 1728.17, 1652.62, 1247.71, 1179.89, 1093.61, 831.20, 774.94, 668.00. GPC molecular weights: Mn = 10500g/mol, Mw = 15700 g/mol, and Mw/Mn =1.5

Other block copolymers PCL_{50}-*b*-$SiPCL_{25}$ and PCL_{50}-*b*-$SiPCL_{50}$ were synthesized varying the M/I ratios.

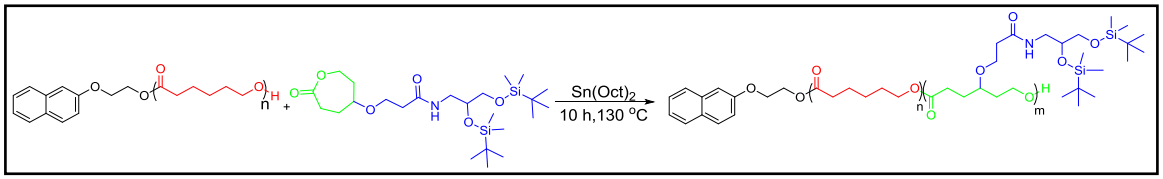

Scheme 2.13

b) Synthesis of PCL-*b*-HyPCL: PCL_{50}-*b*-$SiPCL_{10}$ (250 mg, 49 mmol) was dissolved in a mixture of 5 mL dry THF and 5 mL dry methanol, TBAF in 1 M THF (1.48 mL, 1.48 mmol) was then added drop wise at 0 °C and then the reaction mixture was stirred for 24 h at 25 °C, the reaction mixture was then quenched using 1N HCl. The entire amount of solvent was evaporated and the polymer was purified by dialysis.

^{1}H -NMR (400 MHz, $CDCl_3$) δ ppm: 7.75 (m, 0.06 H), 7.44 (m, 0.02 H), 7.36 (m, 0.02 H), 7.15 (m, 0.04 H), 6.20 (s, 1 H), 4.49 (t, 0.03 H), 4.30 (t, 0.03 H), 4.13 (t, 2 H), 4.07 (t, 2H), 3.80 (m, 1 H), 3.70 (m, 2 H), 3.54 (m, 2 H), 3.39 (m, 3 H), 2.40 (m, 4 H), 2.3 (t, 2H), 1.78 (m, 4 H), 1.62 (m,4H), 1.36 (m, 2H). FT-IR (cm^{-1}): 3431.07, 3369.05, 2940.49, 2866.34, 1719.96, 1646.55, 1364.78, 1237.85, 1171.44, 1041.04, 958.57, 728.00

GPC molecular weights: Mn = 6300, Mw = 10000, and Mw/Mn = 1.6

Similarly, other block copolymers PCL_{50}-*b*-$SiPCL_{25}$ and PCL_{50}-*b*-$SiPCL_{50}$ were deprotected to give block copolymers PCL_{50}-*b*-$HyPCL_{25}$ and PCL_{50}-*b*-$HyPCL_{50}$.

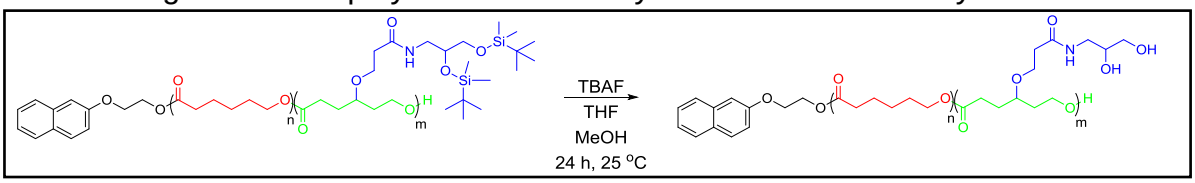

Scheme 2.14

2.3. Self-assembly of polymers

In a typical procedure, 5 mg of polymer was dissolved in 2 ml DMSO, 3 ml water was added dropwise at moderate stirring, further stirred for 4 h at 25^{0}C, then transferred to a

dialysis tube (MWCO = 1000 or 3500) and dialyzed against water. Water was replenished at regular intervals for the removal of DMSO and hence facilitate self-assembly of the polymers.

2.4. Doxorubicin encapsulation in block copolymers.

Doxorubicin, commercially available as DOX.HCl was first neutralized by 5 equivalents of triethyl amine by taking in 0.5 ml of DMSO. 5 mg of the polymer was dissolved in 1.5 ml DMSO and the neutralized DOX in DMSO was added to it. 3 ml water was added dropwise at moderate stirring and then stirred for 4 h at 25^0C. Polymer solution with the drug was then transferred to a dialysis tube (MWCO = 1000 or 3500) and dialyzed against water. Fresh water was replenished for the removal of non-encapsulated DOX and DMSO. The drug loading content (DLC) and drug loading efficiency (DLE) were determined by UV visible spectroscopy using the following equation.

DLC = [weight of encapsulated DOX/Weight of the polymer] x 100 %

DLE = [weight of encapsulated DOX/Weight of the DOX in the feed] x 100 %

2.5. CMC determination using Nile red probe.

Different concentrations of the dialyzed polymer solutions were made in water and transferred to vials containing Nile red dye maintained at 0.2 µM concentration. These solutions were sonicated for 5 h and let to equilibrate at room temperature for 12 h. Fluorescence spectra were recorded and the maximum intensity was plotted against polymer concentration.

2.6. Polymer degradation studies by DLS

Degradation of the polymers in PBS buffer in the presence and absence of esterase enzyme were studied. A 0.6 ml of dialyzed polymer solution in water was taken in 1.2 ml PBS buffer and was slowly stirred at 37^0C. At specific intervals, 1 ml of the solution was taken and DLS readings were measured in order to see the change in size and the solution was transferred back. For esterase aided degradation studies 10 U of the enzyme was used.

2.7. Cell Viability Assay (MTT Assay).

The cytotoxicity of polymers alone was tested in MCF 7 breast cancer cell lines using the tetrazolium salt, 3-(4,5-dimethylthiazol-2-yl)-2,5-diphenyltetrazolium bromide (MTT).10^3 cells were seeded in each well of a 96 well plate in 100 µL of DMEM with 10% FBS (fetal

bovine serum) and was left for 16 h to adhere. Media from each well was removed and then cells were treated with nascent scaffolds varying the concentrations. DMEM with FBS alone was used as a control for all experiments. Cells were incubated for 72 h without changing the media, then the compound containing media was aspirated. A freshly prepared 100 µL of MTT (0.5 mg/ml) was added to each well and the cells were incubated for 4 h at 37 °C. After that the media was aspirated and the purple formazan crystals formed because of the reduction of MTT by the mitochondrial dehydrogenase enzyme were dissolved in 100 µL of DMSO. The absorbance was immediately measured using the microplate reader at 570 nm (Variaskan Flash).

2.8. Cellular uptake of doxorubicin loaded nanoscaffolds by confocal Microscopy

MCF 7 cell lines were seeded at a density of 10^5 cells on coverslips placed in 6 well plates containing DMEM media with 10% FBS and then incubated for 16 h at 37 °C. Cells were treated with DOX alone and DOX loaded micelles for 9 h in a CO_2 incubator at 37 °C. Drug containing media was then aspirated and cells were washed twice with 1 ml PBS and fixed with 4% paraformaldehyde solution in PBS for 15 min at 4 ^oC. Then washed with 1 ml PBS twice and the cells were stained with DAPI solution in PBS for 2 min under dark at rt, excess dye was washed from the plate using PBS, and the cells were gently rinsed with PBS for 1 min, then stained with 500 µl of phalloidin (Alexa fluor 488) for 15 min at 4 ^oC and washed twice with PBS. Coverslips were mounted onto the slides using 70% glycerol medium and then dried overnight at room temperature in the dark. LSM 710 confocal microscope was used to record the images. The images were analyzed using ImageJ software.

2.9. Flow Cytometry Measurements

Flow cytometry analysis was carried out to study the cellular uptake of polymeric micelles in HeLa cell line. 10^5 HeLa cells were seeded in 6 well plate containing DMEM media and incubated for 16 h at 37 °C. The cells were treated with the nano scaffolds and free dox maintaining drug concentration at 2 µg/ml and incubated for 4 h. Then the cells were washed with PBS and digested with 500 µL of trypsin and again incubated for 1 min. The suspension was centrifuged at 1000 rpm for 5 min and pellet was resuspended in 0.5 ml PBS. Flow cytometry studies were conducted using BD LSR Fortessa SORP cell analyzer equipped with five lasers and 18 color detectors.

3. Results and Discussion

3.1. Polymer synthesis and characterization

3.1.1. Monomer synthesis and characterization

A new *γ* substituted caprolactone monomer containing silyl protected hydroxyl groups was designed using a multi-step procedure as shown in scheme 3.1. 1,4-Cyclohexanediol and t-butyl acrylate underwent Michael addition to yield **1**, which was further oxidized to the cyclohexanone derivative **2** using PCC as an oxidizing agent, which was then deprotected using TFA to give acid **3.** Simultaneously two hydroxyl groups in 3-chloropropane-1,2-diol were protected by silyl groups to give **4**, which was then converted to azide to yield **5** and then reduced to amine using Staudinger reaction to get **6**. Compound **3** was coupled to **6** using EDC coupling reagent to yield **7** which further underwent Baeyer Villiger Oxidation to form the substituted caprolactone monomer SiCL **8.** All intermediate products were confirmed by ^{1}H NMR, ^{13}C NMR, HRMS and FTIR.

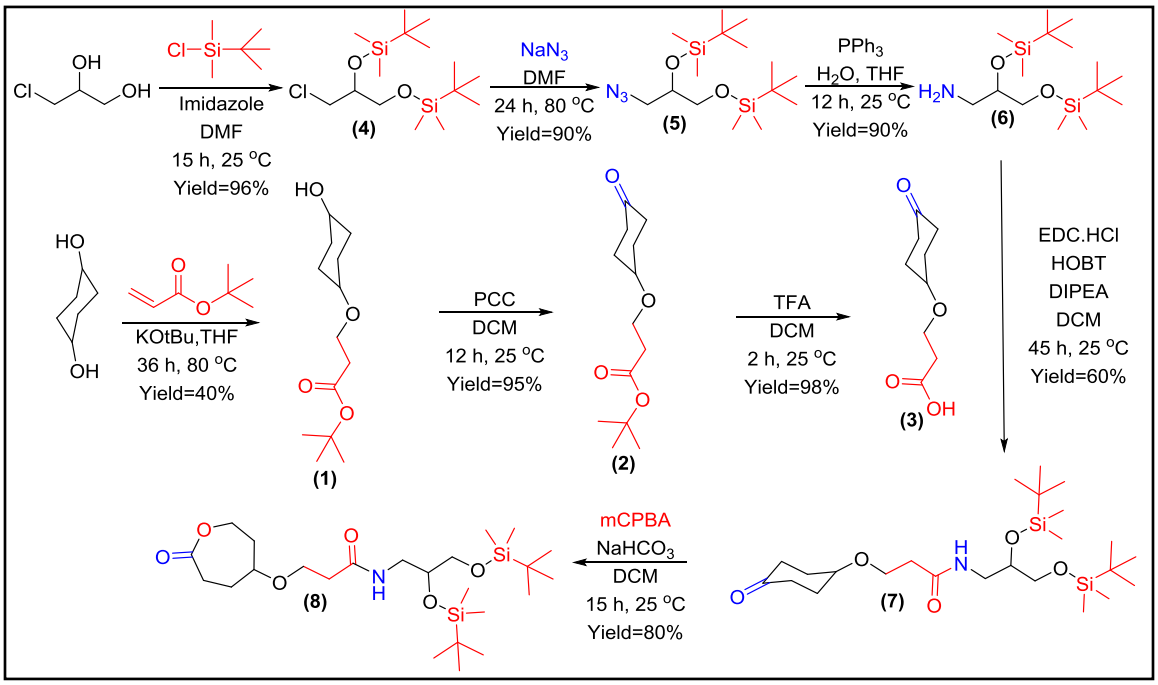

Scheme 3.1: Synthetic scheme for monomer SiCL (8).

^{1}H NMR spectra of compounds **1**, **2** and **3** are shown in figure 3.1, 'H_b' (proton b) of compound **1** shows 2 separate peaks because of cis trans isomers present in the starting material 1,4-cyclohexanediol. Formation of compound **2** after oxidation by PCC was confirmed by the disappearance of the peak 'b' in compound **1.** After the deprotection of

acid group in compound **2,** compound **3** is obtained which was confirmed by the disappearance of peak ‘e’ corresponding to the tertiary butyl group in the acid protecting group and by the appearance of the carboxylic acid peak ‘f’ at 9.44 ppm.

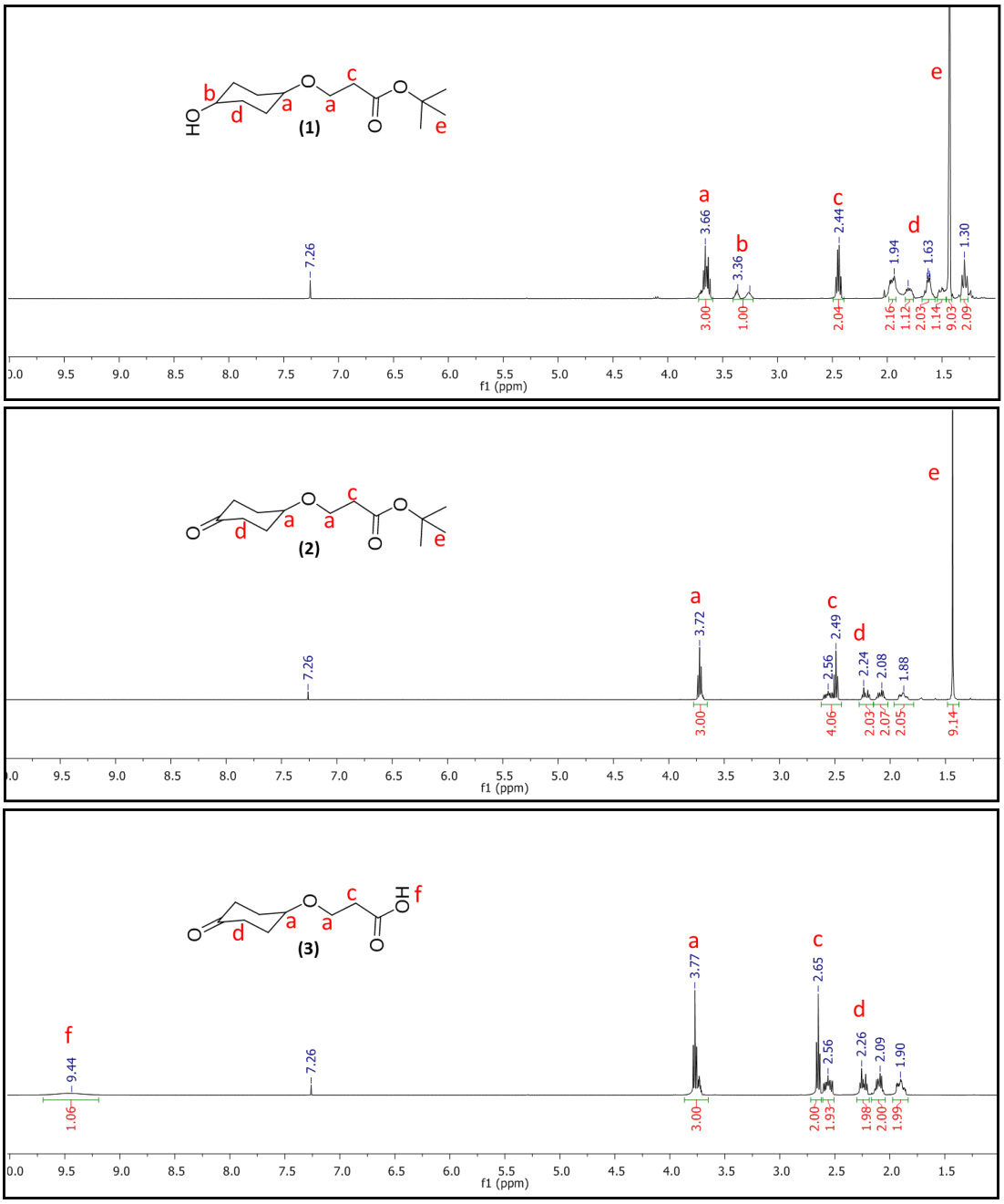

Figure 3.1: ^{1}H NMR spectra of compounds 1, 2 and 3

Figure 3.2 shows the ^{1}H NMR spectra of compounds **4**, **5** and **6,** TBDMS protection of the hydroxyl groups in 3-chloropropane-1,2-diol was confirmed by the appearance of the two peaks ‘k’ and ‘l’ at 0.9 ppm and 0.09 ppm belonging to the TBDMS protecting group. ‘g’

being a chiral center, adjacent protons ‘i’, ‘j’ and ‘h’ become diasterotopic giving rise to multiple peaks and multiplets. When compound **4** is converted to azide **5** peaks ‘l’ and ‘j’ become more shielded as azides are less electron withdrawing than Cl. When azide was reduced to amine to give compound **6,** peaks ‘l’ and ‘j’ get further shielded. Moreover, appearance of amine peak ‘m’ at 1.3 ppm confirms the formation of compound **6.**

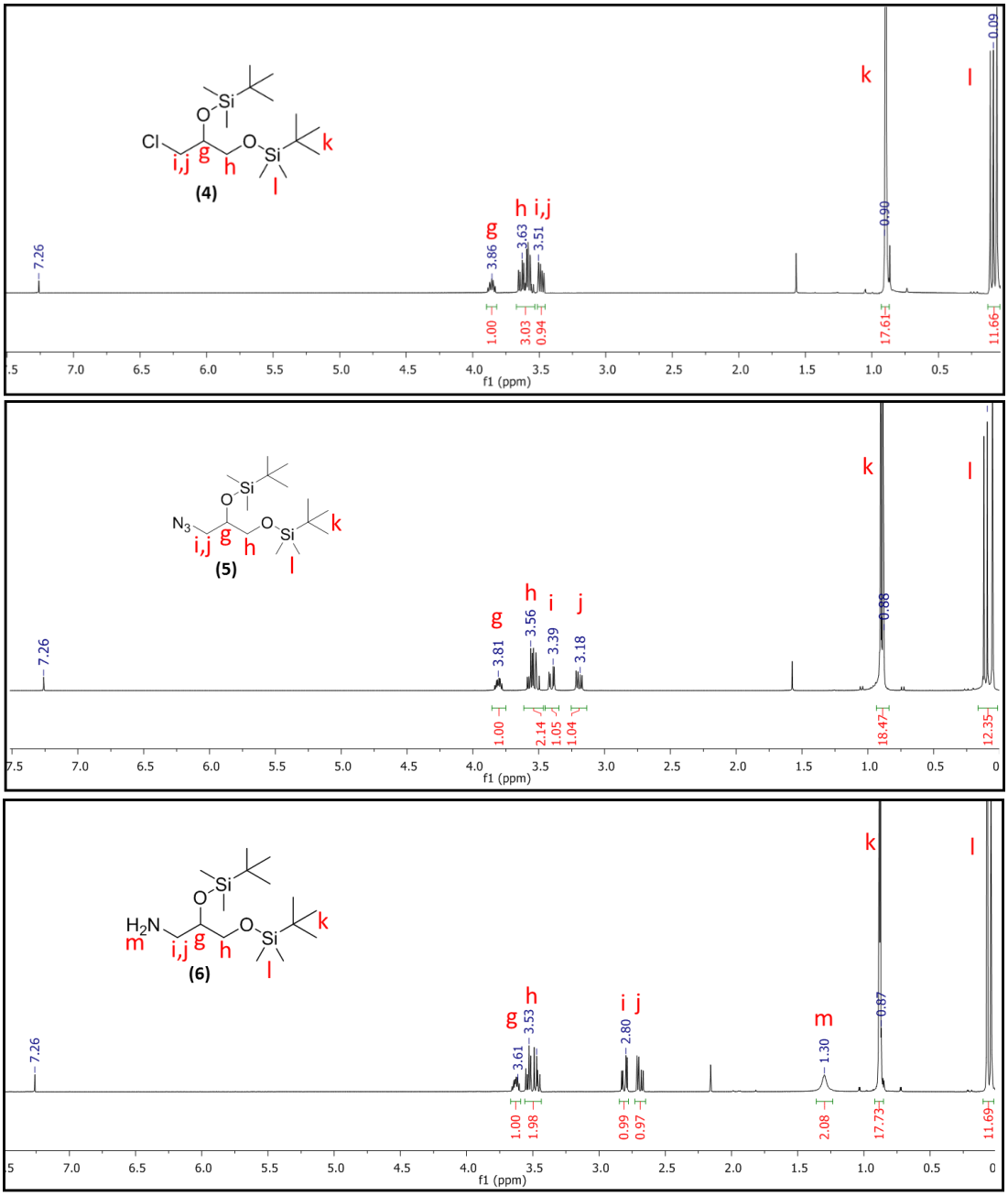

Figure 3.2: ^{1}H NMR spectra of compounds 4, 5 and 6

Formation of compound **7** after the coupling reaction of **3** and **6** was confirmed by the appearance of the amide peak 'n' at 6.2 ppm as shown in figure 33. Amide being more electron withdrawing than amine, peaks 'l' and 'j' gets deshielded in compound **7.** Upon Baeyer Villiger reaction of **7** the monomer SiCL was formed, peaks 'd' belonging to the cyclohexane ring vanishes completely giving rise to new peaks 'o, p, q, r, s' belonging to the caprolactone ring (figure 3.3).

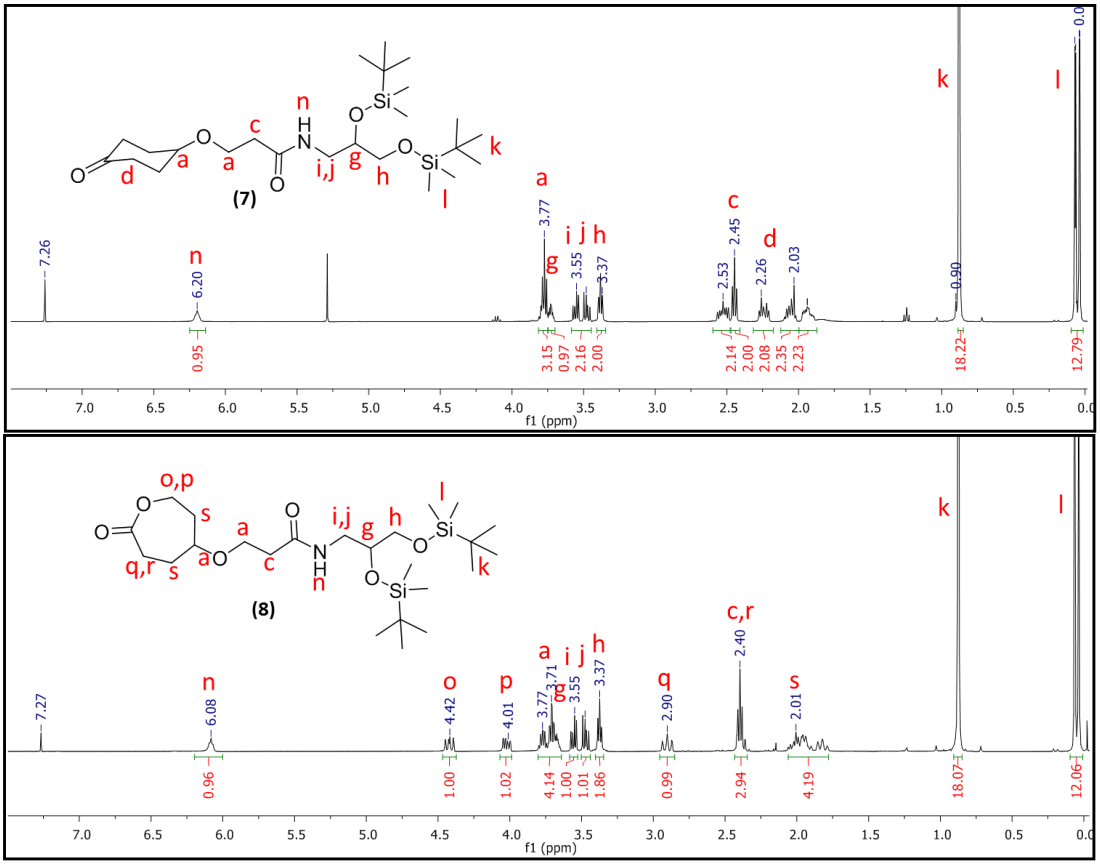

Figure 3.3: ^{1}H NMR spectra of compounds 7 and 8

3.1.2. Initiator synthesis and characterization.

A new UV active initiator NAP-OH (**9**) based on Naphthalene was designed by the reaction of 2-Naphthol with bromoethanol (Scheme 2.9). ^{1}H NMR peaks are assigned based on the electron donating nature of oxygen and peak splitting pattern obtained (figure 3.4).

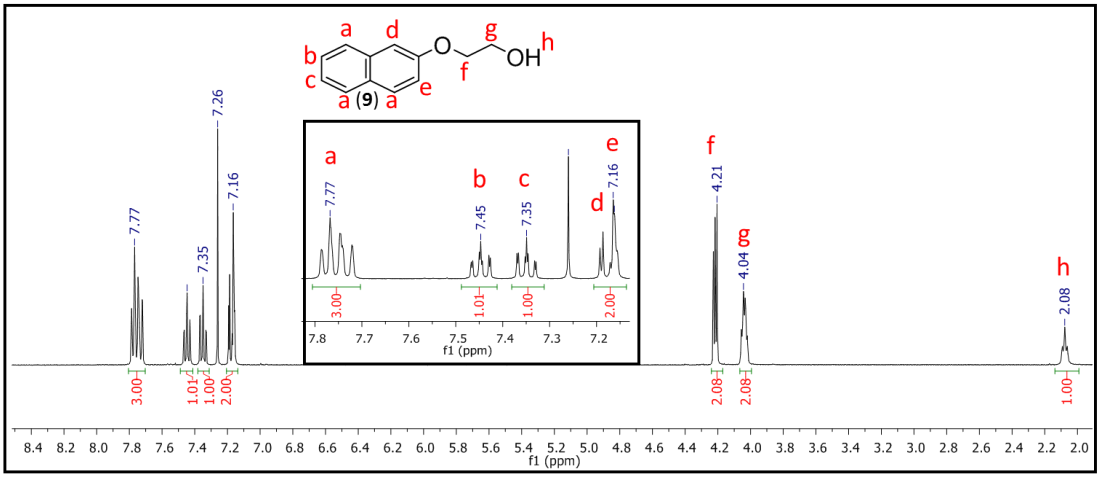

Figure 3.4: ^{1}H NMR spectra of NAP-OH (9).

3.1.3. Homopolymer synthesis and characterization

Caprolactone monomer SiCL (**8**) underwent Ring opening polymerization with the initiator NAP-OH (**9**) in the presence of $Sn(Oct)_2$ catalyst following the melt route under solvent free conditions to give SiPCL polymer (scheme 3.3). $Sn(Oct)_2$ follows coordination insertion mechanism for ROP as shown in scheme 3.2.

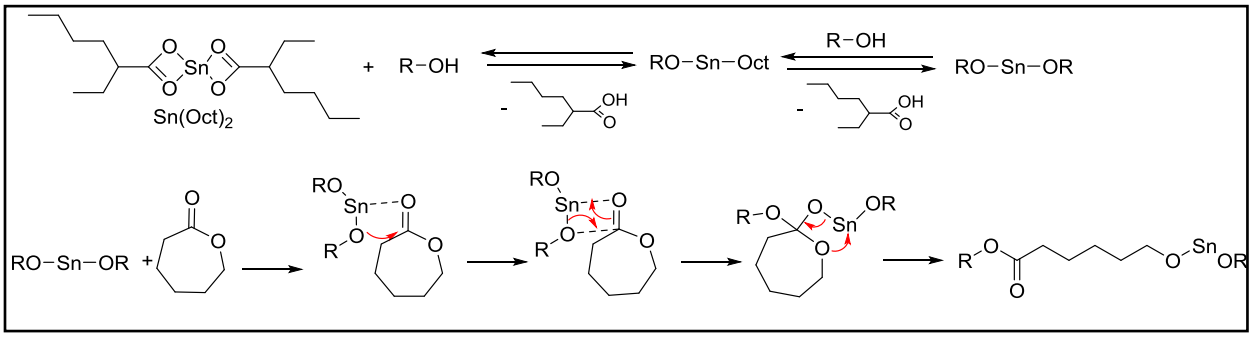

Scheme 3.2: ROP mechanism of $Sn(Oct)_2$ catalyst

ROP being a controlled polymerization technique, three different homopolymers of this monomer were synthesized with monomer repeating units 10, 50 and 100 varying the monomer to initiator ratio. SiPCL polymers are highly hydrophobic, so hydroxyl groups on their branches were deprotected to give HyPCL polymers having hydroxyl pendant groups, making the polymers completely hydrophilic, hence water soluble and a good replacement for poly ethylene glycol (PEG) which is routinely used as a hydrophilic block. Moreover, functional hydroxyl groups can be used to conjugate targeting ligands, drug molecules and fluorophores.

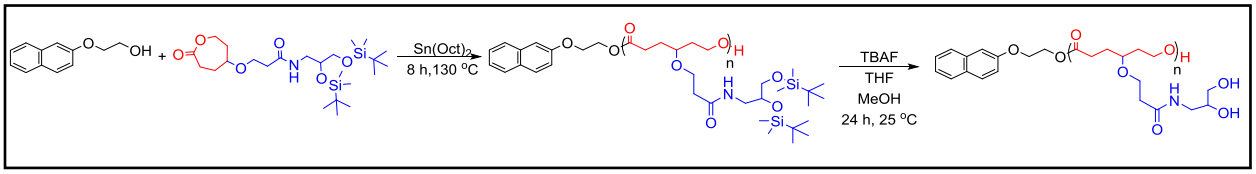

Scheme 3.3: Synthesis of SiPCL and its deprotection to give HyPCL.

^{1}H NMR spectra of $SiPCL_{10}$ and $HyPCL_{10}$ in CD_3OD solvent is shown in figure 3.5. Number average degree of polymerization (DPn) was determined from ^{1}H-NMR comparing the proton at 7.4 ppm (proton 'a') of the initiator NAP-OH and proton at 4.14 ppm (proton 'd') from SiPCL part. For this case, the DPn value was obtained from ^{1}H NMR as 10 units for the feed ratio of M/I = 10; giving the integration 2 for 'a' gives 20 for 'd'. Table 3.1 shows the DPn and number average molecular mass (Mn) of the homopolymers synthesized. The deprotection of this polymer using TBAF was confirmed by the disappearance of the peaks at 0.9 ppm (proton 'k') and 0.08 ppm (proton 'l') which corresponds to the silyl protecting group.

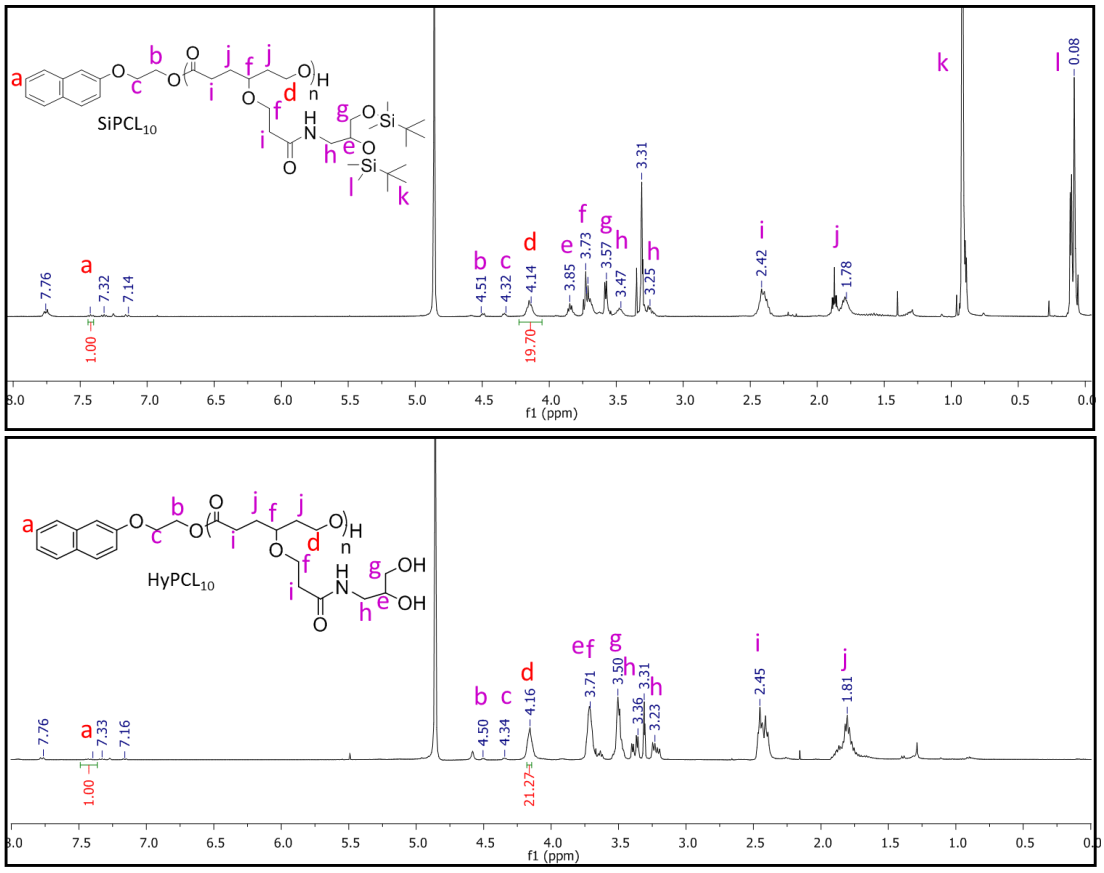

Figure 3.5: ^{1}H NMR spectra of the polymers $SiPCL_{10}$ and $HyPCL_{10}$

Gel permeation chromatography (GPC) or size exclusion chromatography is a powerful characterization technique which will give weight average molecular weight (Mw), number average molecular weight (Mn) and Polydispersity index (PDI), which is important to know the purity of the polymers. GPC chromatograms of the are shown in Figure 3.6. GPC three SiPCL polymers of the polymers performed in THF using polystyrene standards gave monomodal distribution with narrow PDI. Mn, Mw and PDI of these polymers are listed in table 3.1. Mn and Mw were under estimated because the standardization was done using polystyrene. GPC of HyPCL homopolymers were unable to record because of their insolubility in THF.

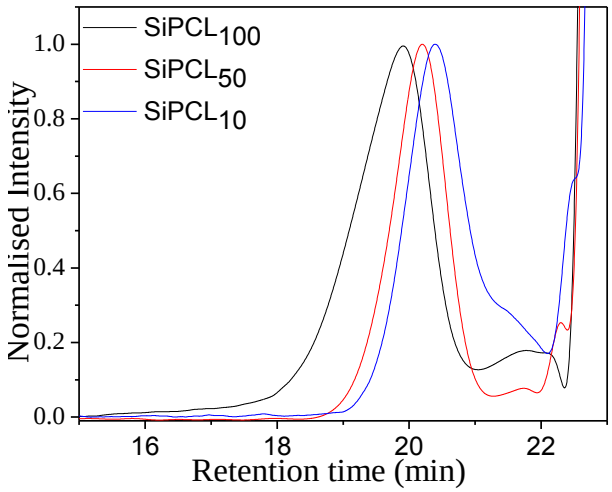

Figure 3.6: GPC chromatograms of SiPCL polymers

SI NO	Polymer	NMR			GPC		
		DPn		Mn (g/mol)	Mn (g/mol)	Mw (g/mol)	PDI
		Feed	Incorporated				
1	$SiPCL_{10}$	10	10	5200	3900	4800	1.2
2	$SiPCL_{50}$	50	49	24900	6200	7400	1.2
2	$SiPCL_{100}$	100	98	50381	8800	11700	1.3

Table 3.1: ^{1}H NMR and GPC characterization table of SiPCL polymers.

MALDI of $SiPCL_{10}$ and $HyPCL_{10}$ were recorded and is shown in figure 3.7. MALDI confirms that ROP was initiated by the initiator NAP-OH and initiator remains intact after deprotection of the hydroxyl groups. MALDI of SiPCL showed a single distribution with separation between the peaks 504 corresponding to SiCL monomer. MALDI of HyPCL showed two distributions, one sodiated and the other potassiated with separation between the peaks 275 corresponding to SiCL monomer after hydroxyl deprotection

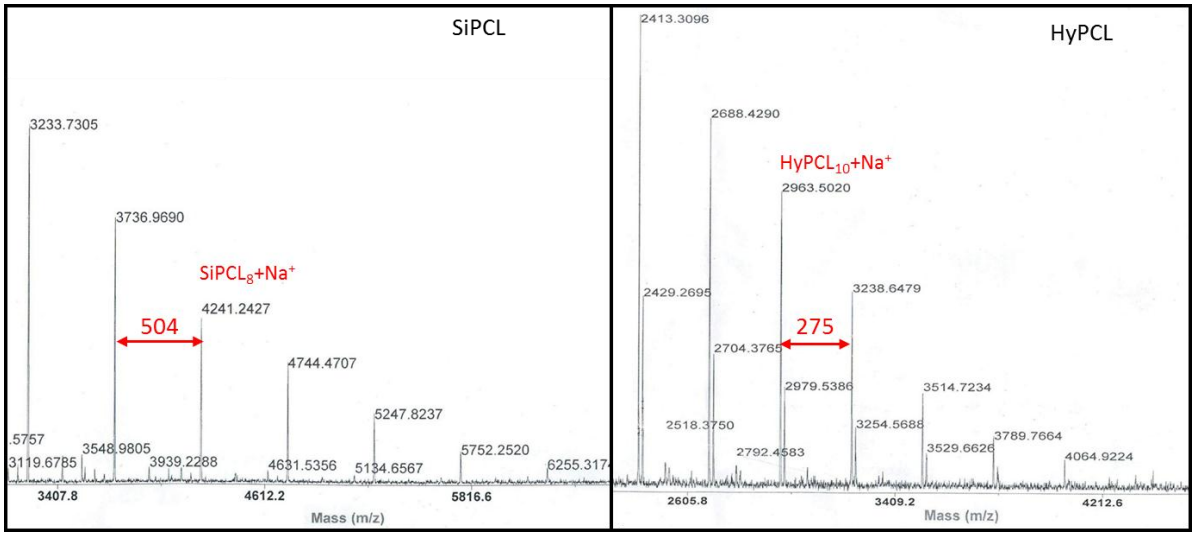

Figure 3.7: MALDI of SiPCL and HyPCL

3.1.4. Synthesis of block copolymers and their characterization

The synthesis of the block copolymers was done using a new method, in which the first block was synthesized by ROP and purified initially, which was further used as a macro initiator for the second block. Scheme 3.4 shows the synthetic strategy for PCL-*b*-HyPCL which was obtained by the deprotection of the block copolymer PCL-*b*-SiPCL. Number average degree of polymerization (DPn) in the macro initiator PCL was determined by comparing protons at 7.4 ppm (proton 'a') of the initiator and 4.05 ppm (proton 'd') from the PCL part. For the feed ratio of M/I = 50, DPn value was obtained from ^{1}H-NMR as 50 units. Further, the DPn of the next block SiPCL was obtained using the protons 'd' of the macro initiator NAP-PCL and 'i' at 4.14 ppm from the new block SiPCL, giving the DPn value as 50 as given in the feed. The deprotection of hydroxyl groups in PCL-*b*-SiPCL to give PCL-*b*-HyPCL was confirmed by the disappearance of the peaks at 0.87 ppm (proton 'g') and 0.08 ppm (proton 'h') belonging to TBDMS protecting groups (figure 3.8). Similarly, two different blocks were synthesized keeping the PCL block constant and varying the number of SiCL monomer units 25 and 50. DPn and number average molecular weights of the three polymers PCL-*b*-SiPCL and the deprotected polymers PCL-*b*-HyPCL are shown in table 3.2. Deprotected block copolymers containing hydroxyl groups where readily dispersible in water.

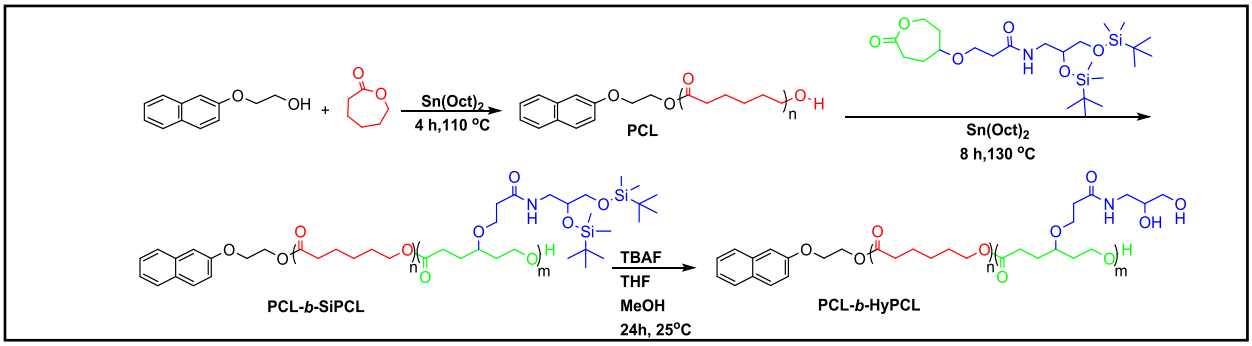

Scheme3.4: synthesis of PCL-b-SiPCL and its deprotection to give PCL-b-HyPCL.

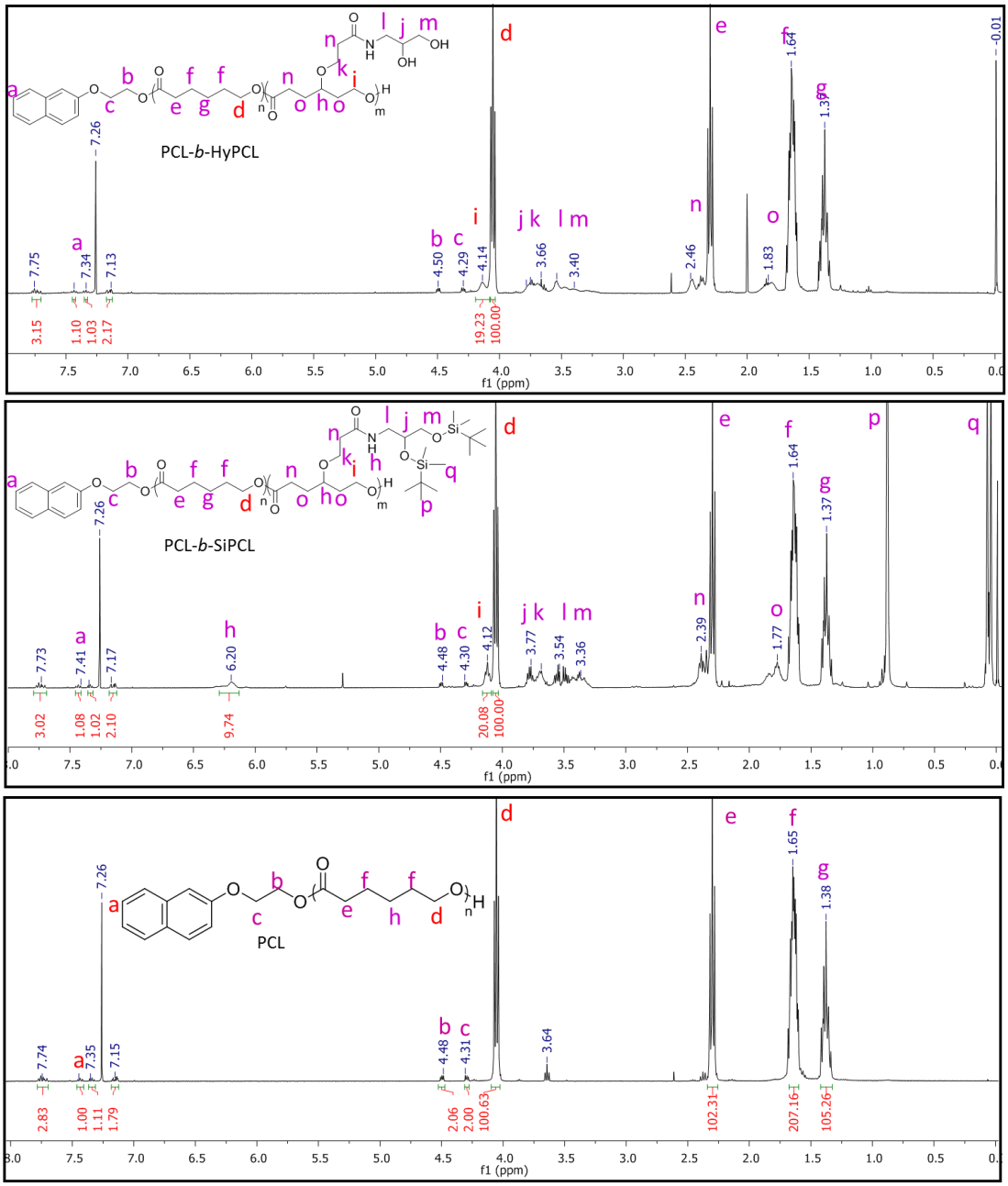

Figure 3.8: ^{1}H NMR of the macro initiator PCL, block copolymers PCL-*b*-SiPCL, PCL-*b*-HyPCL

MALDI of the macro initiator PCL_{50} was recorded to confirm that ROP was initiated by NAP-OH. MALDI showed two distributions belonging to sodiated and potassiated peaks, with a separation between the peaks 114, corresponding to the caprolactone monomer (figure 3.9).

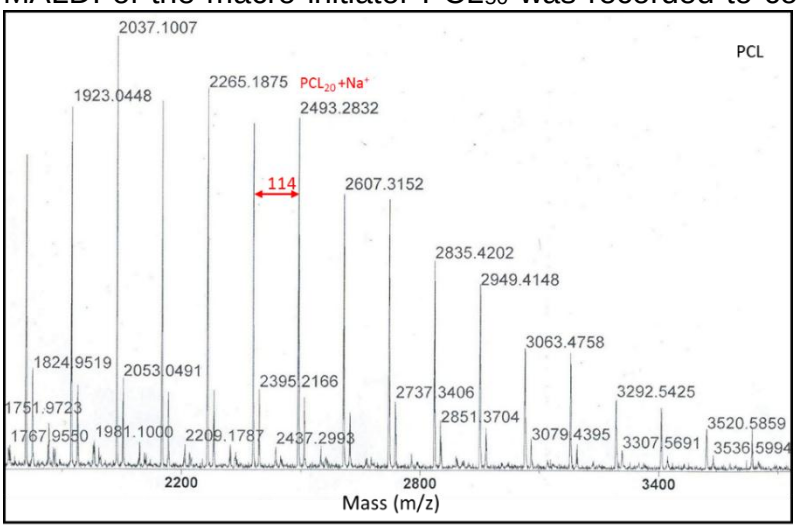

Figure 3.9: MALDI spectra of PCL_{50}

GPC chromatograms of the macro initiator PCL_{50}, block copolymer PCL_{50}-*b*-$SiPCL_{10}$ and deprotected block copolymer PCL_{50}-*b*-$HyPCL_{10}$ are shown in Figure 3.10. GPC of the polymers performed in THF using polystyrene standards gave monomodal distribution with narrow PDI. Mn, Mw and PDI of all the polymers are listed in table 3.2. The increase in molecular weight after forming the block copolymer from the macro initiator PCL_{50} is clearly visible in the GPC chromatograms, and when the hydroxyl groups on this block polymer were deprotected, the molecular weight get decreased and hence eluted at a higher retention time in GPC. Mn and Mw were under estimated because the standardization was done using polystyrene. GPC of PCL_{50}-*b*-$HyPCL_{50}$ block copolymer was unable to measure because of its insolubility in THF.

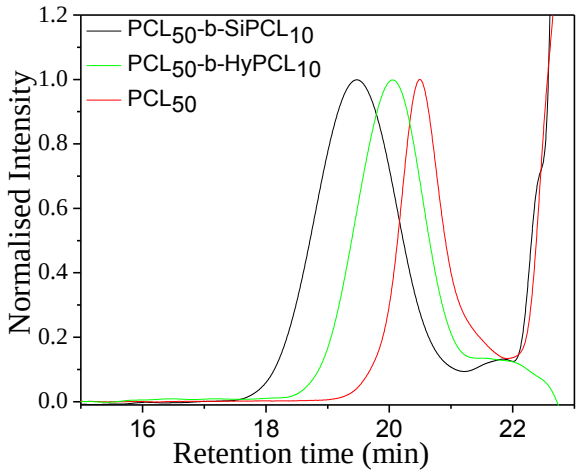

Figure 3.10: GPC chromatograms of the polymers PCL_{50}, PCL_{50}-*b*-$SiPCL_{10}$ and PCL_{50}-*b*-$HyPCL_{10}$

To prove the controlled ROP process, ROP kinetics was performed for the macro initiator and the block copolymer PCL_{50}- *b*-$SiPCL_{50}$. Aliquots were taken at regular intervals, ^1H NMR and GPC were recorded. ^1H NMR spectra of the aliquots for PCL is stack plotted in figure 3.11 a. As time proceeds the intensity of monomer peaks decreases (as marked

SI NO	Polymer	NMR			GPC		
		DPn		Mn (g/mol)	Mn (g/mol)	Mw (g/mol)	PDI
		Feed	Incorporated				
1	PCL_{50}	50	50	5900	5400	6500	1.2
2	PCL_{50}-*b*-$SiPCL_{10}$	10	10	10900	10500	15700	1.5
3	PCL_{50}-*b*-$SiPCL_{25}$	25	24	18000	11300	15100	1.4
4	PCL_{50}-*b*-$SiPCL_{50}$	50	47	29600	12600	16100	1.3
5	PCL_{50}-*b*-$HyPCL_{10}$	----	----	8650	6300	10000	1.6
6	PCL_{50}-*b*-$HyPCL_{25}$	-----	----	12500	8700	11700	1.4
7	PCL_{50}-*b*-$HyPCL_{50}$	----	----	18800	----	----	----

Table 3.2: ^{1}H NMR and GPC characterization of the block copolymers and the macro initiator

for example, peak 'W' in figure 3.11 a) and the polymer peak appears (Peak X). For this polymer, the Mn determined by the ^{1}H NMR showed an increasing trend with polymerization time, hence the occurrence of the controlled ROP process was confirmed (figure 3.11 e). The same was observed for PCL_{50}-*b*-$SiPCL_{50}$, as polymerization time proceeded peaks of the monomer SiCL decreased (eg: peak Y) and the polymer peaks intensity increased (eg: peak Z) (Figure 3.11 b). GPC chromatograms for both the kinetics experiment showed significant change in the retention time and the PDI remained a constant supporting the controlled nature of ROP.

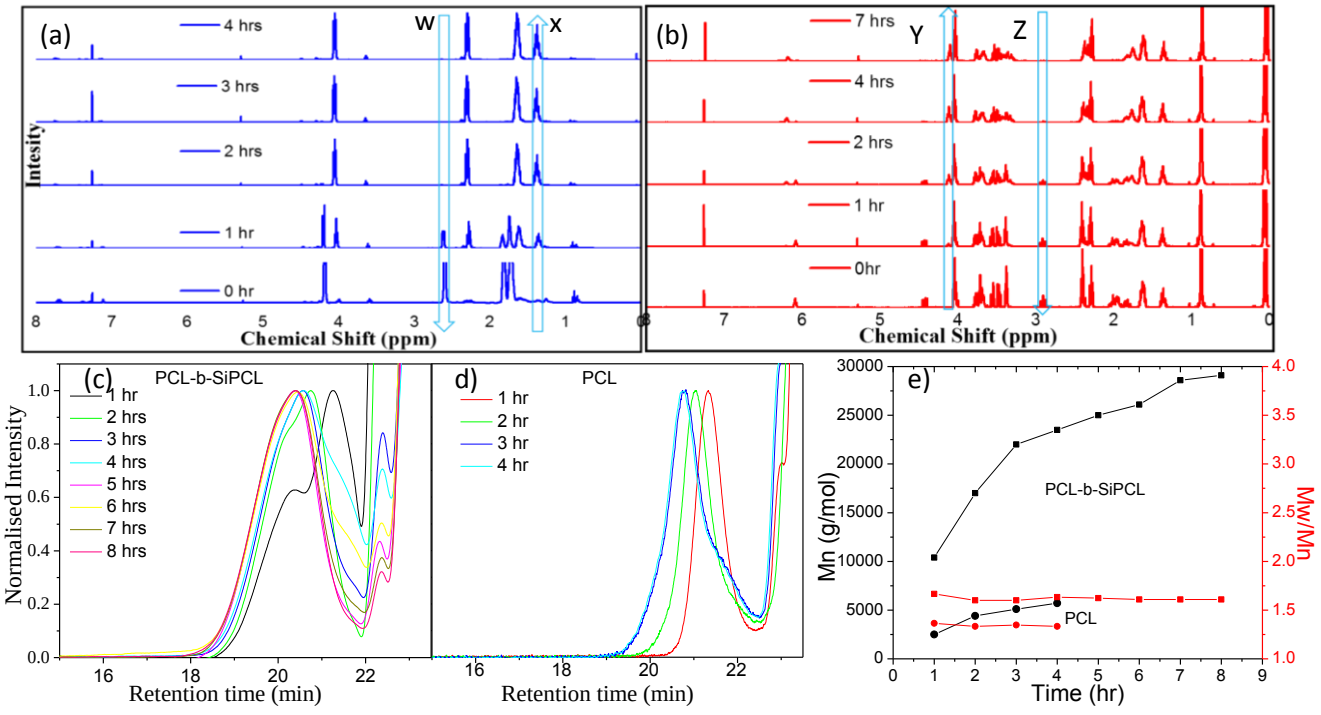

Figure 3.11: ROP kinetics experiment of a) PCL_{50} and b) PCL_{50}- *b*-$SiPCL_{50}$

3.2. Thermal properties of polymers

Thermal stability of the polymers was analyzed using Thermogravimetric analysis (TGA) and they were found to be stable up to 250 ^{0}C. Differential scanning calorimetry (DSC) measurements were conducted in order to check the semicrystalline or amorphous nature of the polymers. Homopolymers SiPCL and HyPCL were completely amorphous. PCL homopolymer was crystalline with melting transition T_m = 52 ^{0}C. The block copolymers PCL-*b*-SiPCL were semicrystalline, and they showed a cold crystallization peak followed by melting transition (Figure 3.12 a,b). Moreover, the enthalpy of melting reduced drastically as shown in the plot c in figure 3.12. The deprotected block copolymers PCL-*b*-HyPCl were also semicrystalline, melting enthalpy reduced with increase in HyPCL units, but the decrease was not much compared to PCL-*b*-SiPCL block copolymers. So, it may be deduced that the bulkiness of the silyl protecting group in the PCL-*b*-SiPCL block led to the decrease in the semicrytalline nature. Polarizing light microscope (PLM) was employed to visualize the nature of chain packing in these semicrystalline polymers. The polymer was heated on a hot stage at 10 ^{0}C/min and images were captured while cooling to record the crystallization process. PCL_{50} crystallized out as spherulites (Figure 3.12 d), similarly other block copolymers PCL_{50}-*b*-$HyPCL_{10,25}$ formed smaller spherulites, whereas PCL_{50}-*b*-$HyPCL_{50}$ was sluggish to crystallize.

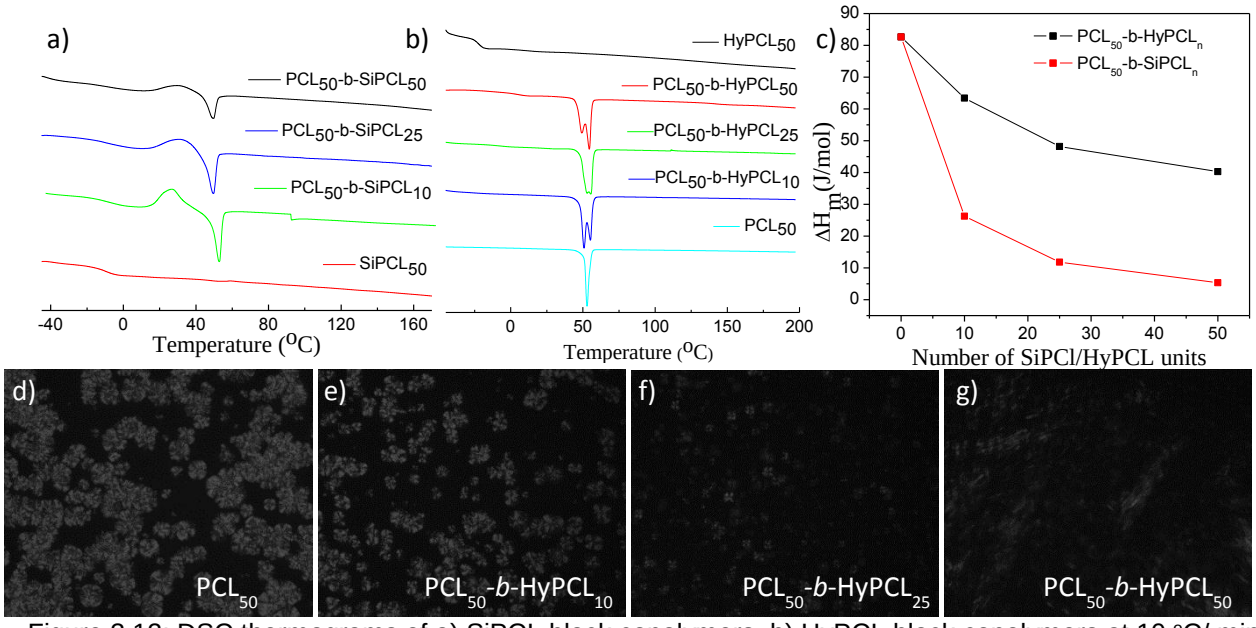

Figure 3.12: DSC thermograms of a) SiPCL block copolymers b) HyPCL block copolymers at 10 ^{o}C/ min in the heating cycle, c) Enthalpy of melting v/s number of monomer units for the block copolymers, PLM images of d) PCL_{50}, e-g) PCL_{50}-*b*-$HyPCL_{n=10,25,50}$ at 10 ^{o}C/min cooling from melt.

3.3. Self-assemblies of polymers

All the three deprotected homopolymers $HyPCL_{n=10,50,100}$ and block copolymers PCL_{50}-*b*-$HyPCL_{n=10,15,50}$ were subjected to self-assembly in water by dialysis method. A typical dialysis setup is shown in figure 3.13 d. PCL back bone acted as the hydrophobic part and the hydroxyl containing branches acted as the hydrophilic part resulting in a collapsed nanoparticle in the homopolymers. Hydroxyl containing PCL block acted as the hydrophilic part while the PCL block brought the hydrophobicity in the block copolymers. Dynamic light scattering (DLS) studies were conducted to understand the self-assembly. All the homopolymers formed clear solutions, and DLS histograms showed monomodal distributions with sizes 200-250 nm as shown in figure 3.13c for the homopolymer with 50 units. The block copolymer with 10 HyPCL units formed a turbid solution, whereas other two block copolymers with HyPCL units 25 and 50 formed clear solutions explaining the hydrophilic character of HyPCL block. DLS studies revealed the presence of two types of nanoparticles in these two systems, one with a smaller size 20-40 nm which may correspond to isolated micelle, while the other with size around 200 nm belonging to the aggregated micelles (figure 3.13 a, b). The morphologies of the two bock copolymers with HyPCL units 25 and 50 were studied using electron microscopy techniques. Field emission scanning electron microscopy (FESEM) images of these two block copolymers are shown in figure 3.13 e, f. They showed spherical nanoforms with size 30-100 nm.

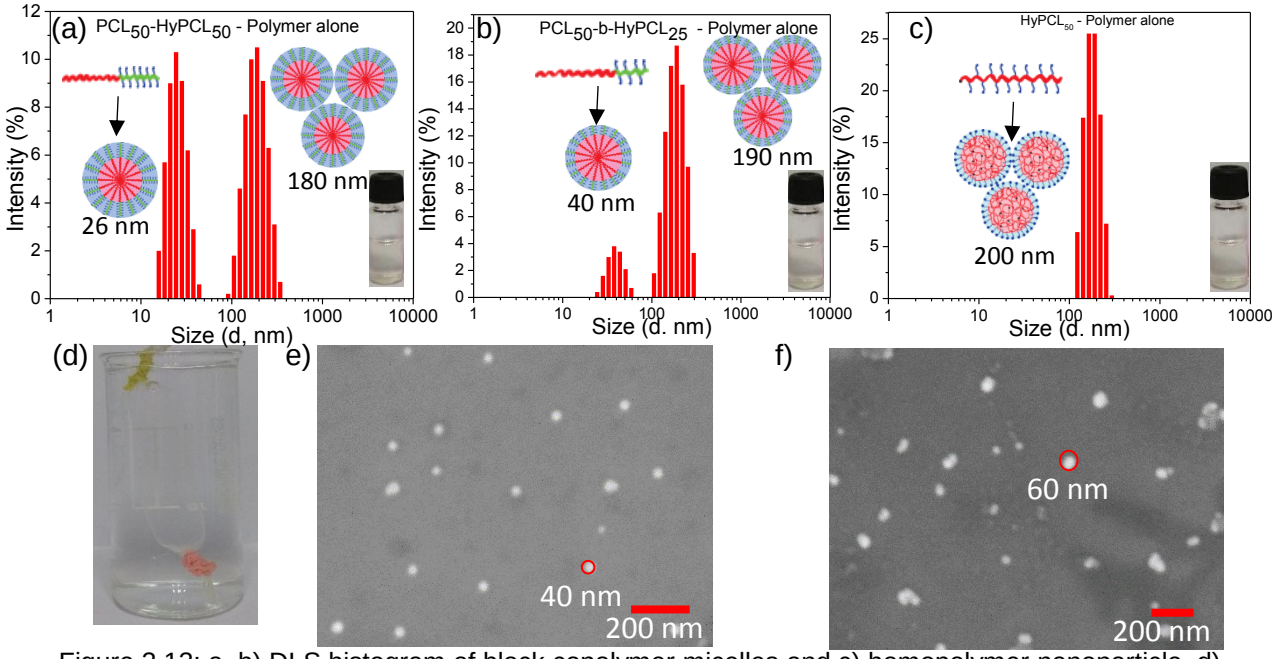

Figure 3.13: a, b) DLS histogram of block copolymer micelles and c) homopolymer nanoparticle. d) dialysis setup. e, f) FESEM images of block copolymer micelles.

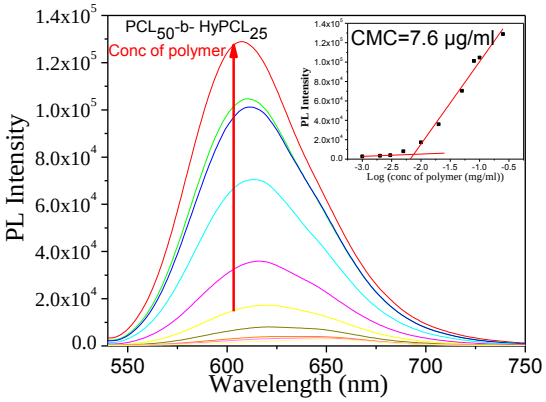

Figure 3.14: CMC determination of the block copolymer NAP-PCL$_{50}$-*b*-HPCL$_{25}$

Critical micellar concentration (CMC) of the homopolymer HyPCL$_{50}$ and the two block copolymers PCL$_{50}$-*b*-HyPCL$_{n=25,50}$ were determined using Nile red dye as a probe. The concentration of Nile red was fixed at 0.2 µM concentration and the polymer concentration was varied. Emission maxima was plotted against the polymer concentration, it was observed that below the CMC there was no Nile red encapsulated, while at CMC Nile red got encapsulated and hence the fluorescent intensity increased, on increasing polymer concentration further, emission intensity increased. The break point is taken as CMC, 7.6 µg/ml for PCL$_{50}$-*b*-HyPCL$_{25}$, 16.4 µg/ml for PCL$_{50}$-*b*-HyPCL$_{50}$ and 195.9 µg/ml for the homopolymer.

To understand the hydrophilic and hydrophobic character of the polymers, Water contact angle (WCA) measurements were done using sessile drop method. Polymer films were made on glass substrates and the images of water drops on them were captured, shown in figure 3.15 along with their water contact angles. The more the WCA the more will be the hydrophobicity. These studies clearly showed the hydrophobic character of non-deprotected polymers having water contact angle more than 90^0 and the hydrophilic nature of the deprotected polymers with WCA less than 50^0.

Homopolymers					Block copolymers				
n	SiPCL$_n$		HyPCL$_n$		n	PCL$_{50}$-*b*-SiPCL$_n$		PCL$_{50}$-*b*-HyPCL$_n$	
	Image	WCA	Image	WCA		Image	WCA	Image	WCA
10	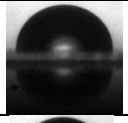	92.4^0	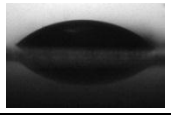	43.2^0	10	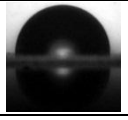	91.1^0	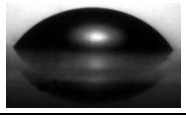	52.9^0
50	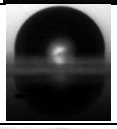	96.1^0	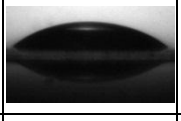	32.3^0	25	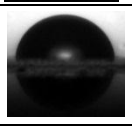	93.1^0	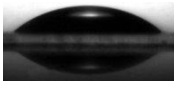	38.8^0
100	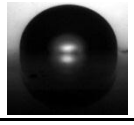	96.5^0	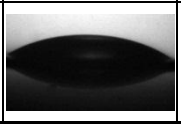	22.3^0	50	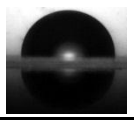	94.8^0	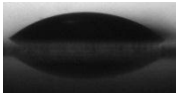	34.1^0

Figure 3.15: Images of water drops on different polymers and their WCA.

3.4. Doxorubicin encapsulation in the polymers

Three homopolymers $HyPCL_{10,50,100}$ and block copolymers PCL_{50}-*b*-$HyPCL_{25,50}$ were subjected to encapsulation of anticancer drug doxorubicin. Homopolymers which were completely water soluble were not able to load DOX, moreover the CMC was found out to be 170-180 µg/ml for them. Two block copolymers encapsulated DOX, Drug loading content (DLC) and drug loading efficiency (DLE) were determined using UV visible spectroscopy, absorbance spectra are shown in figure 3.15 d. DLC = 3.4%, DLE =34% for the block copolymer with 50 HyPCL units and DLC = 2.6%, DLE = 26% for the block copolymer with 25 HyPCL units. The presence hydroxyls on the HyPCL block enhanced DOX loading due to extensive hydrogen bonding. DLS measurements of these DOX loaded nanoparticles were done to ensure the stability of the scaffolds after DOX loading. DLS showed a bimodal distributions similar that of the self-assembled polymer, one with size 20-30 nm and the other with 120- 150 nm (Figure 3.16 b,c). FESEM images revealed the spherical nature of the DOX loaded nano scaffolds with size 30-100 nm (Figure 3.16 e,f).

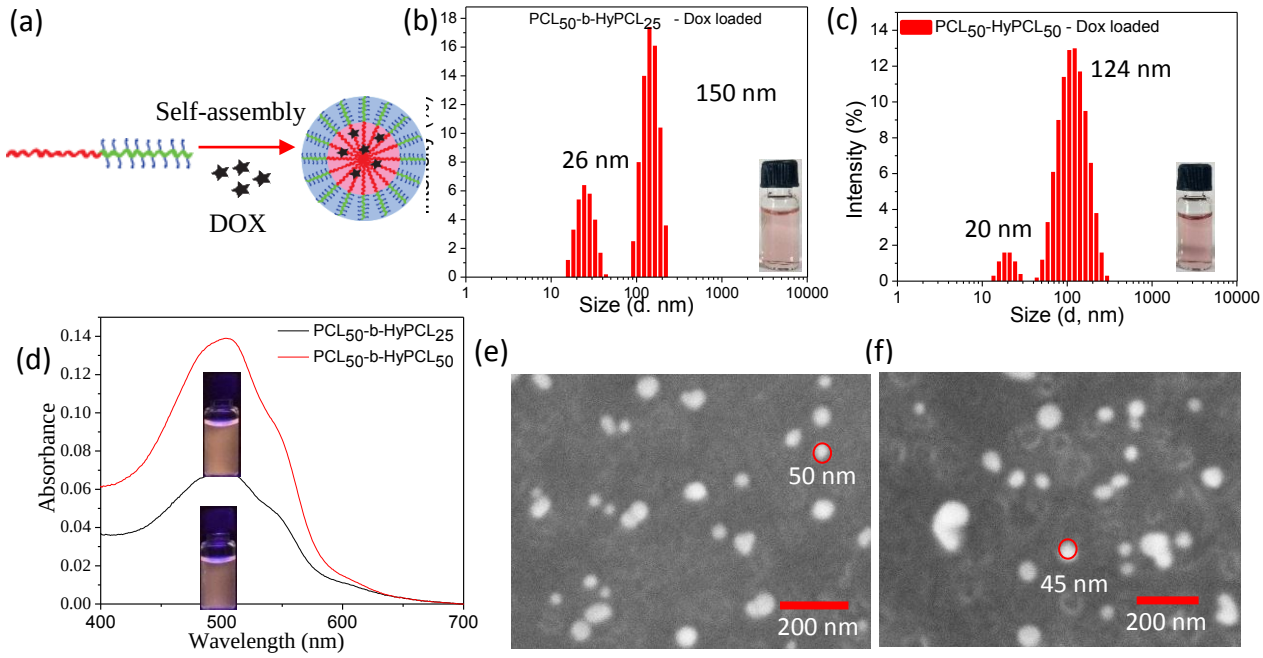

Figure 3.16: a) Schematic representation of Doxorubicin encapsulation by block copolymers. b, c) DLS histogram of DOX loaded micelles of block copolymers. d) absorbance spectra of DOX loaded micelles in water. e, f) FESEM images of dox loaded micelles of block copolymers.

3.5. Polymer degradation studies

Ester bonds in the PCL backbone can be cleaved by esterase enzyme which is found abundantly in the lysosomes. Once the nanoparticles enter the cell, polymer will get chopped by esterase, resulting in the disruption of the nanoparticle, leading to the release of the loaded drug. To check the biodegradability of these polymers, time dependent DLS studies were conducted in the presence of esterase enzyme (figure 3.17 a). Self-assembled polymers were taken and were stirred slowly in PBS buffer, for esterase guided study, 10 U of esterase was used. Polymers were cleaved as time progressed, resulting in turbidity in the solution and hence size obtained from DLS increased. Figure 3.17 b, c shows the size v/s time plot for the two block copolymers, which shows clearly the increase in size as time proceeds and 100% cleaving was observed after 5-7 h in esterase aided degradation.

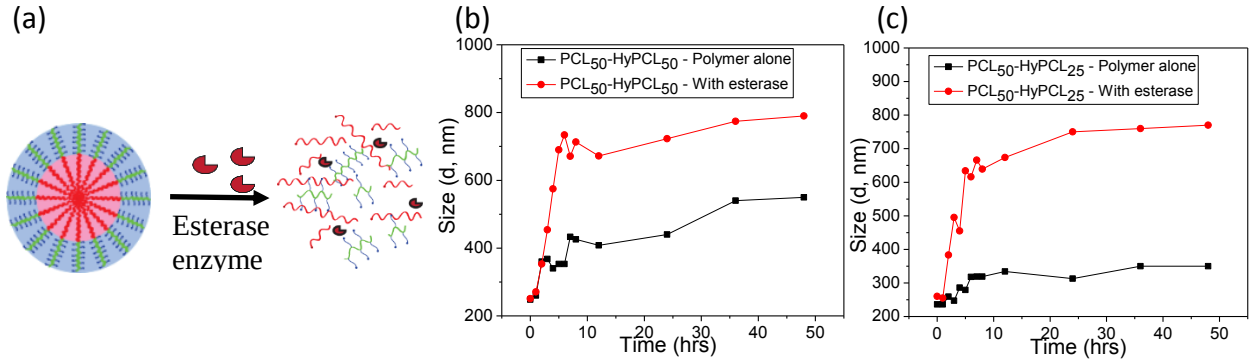

Figure 3.17: Polymer degradation studies by DLS

3.6. Cytotoxicity and cellular uptake

Cytotoxicity of nascent polymeric micelles was examined in MCF 7 breast cancer cell lines. Cytotoxicity of the two block copolymers PCL_{50}-*b*-$HyPCL_{25,50}$ was tested in MCF 7 cell line over a range of concentrations and they were found to be non-toxic to the cells up to 60 µg/ml, the histograms are shown in figure 3.18

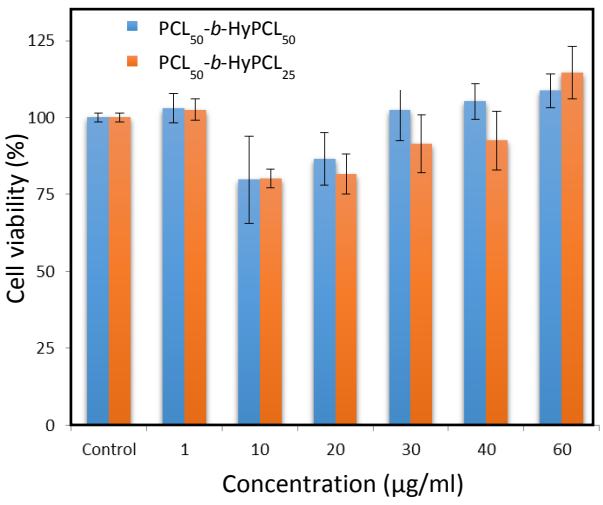

Figure3.18: Cytotoxicity of nascent polymer scaffolds (MTT assay)

Cellular uptake of these nanocarriers was analyzed in MCF 7 cell line. Confocal laser scanning microscopy (CLSM) was used to visualize the cellular uptake of free DOX and DOX loaded nano scaffolds. DAPI was used to stain the nucleus and phalloidin to stain the actins in the cell membrane. DOX, phalloidin stained actins and DAPI stained nucleus were visualized using red (λ=561 nm), green (λ=488 nm) and blue (λ=405 nm) channels respectively (Shown in figure3.19). The first panel corresponding to free DOX shows red fluorescence due to DOX predominantly in the nucleus and negligibly less in the cytoplasm. The second panel (DOX loaded PCL_{50}-*b*-$HyPCL_{50}$) shows that the DOX is mostly adhered to the cell membrane with partially inside the cells, while for DOX loaded PCL_{50}-*b*-$HyPCL_{25}$ (third panel) the drug is distributed all over the cell including the nucleus.

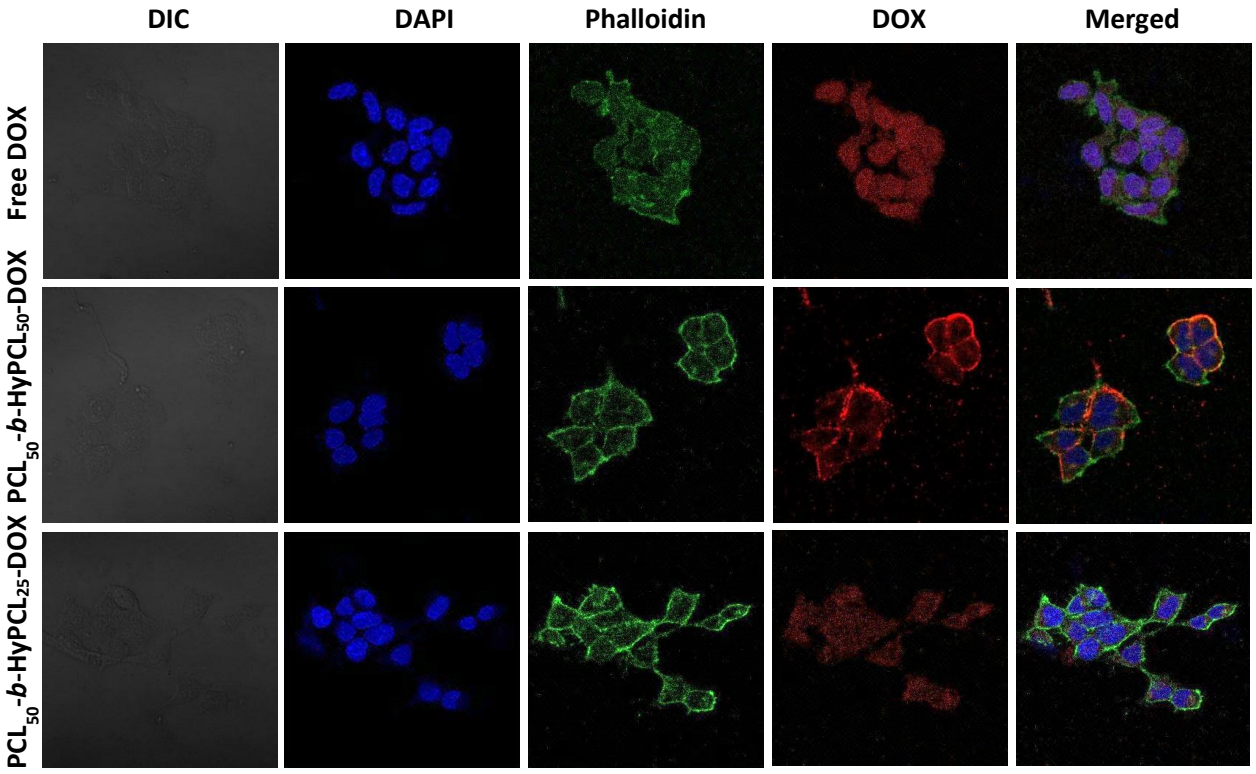

Figure 3.19: Confocal images of MCF 7 cells incubated with free doxorubicin (panel 1), PCL_{50}-*b*-$HyPCL_{50}$-DOX (panel 2) and PCL_{50}-*b*-$HyPCL_{25}$-DOX (panel 3).

Flow cytometric analysis was done to see the cellular internalization of the nanocarriers.

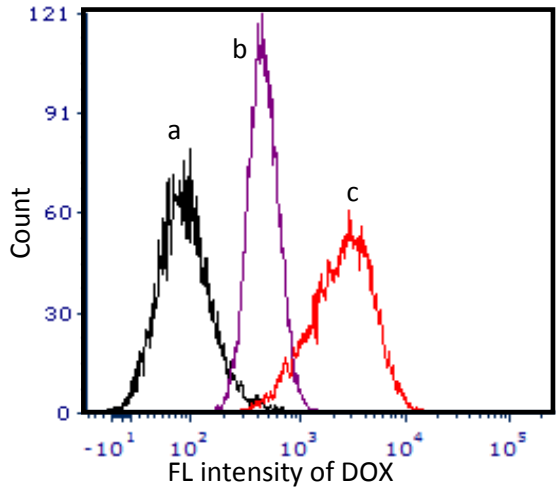

Results (figure 3.20) shows that the cellular uptake of the doxorubicin loaded nanoparticles of the block copolymer PCL_{50}-*b*-$HyPCL_{50}$ was 6 fold higher compared to that of free dox.

Figure 3.20 : Flow cytometric analysis, a) control, b) free DOX and c) DOX loaded PCL_{50}-*b*-$HyPCL_{50}$.

4. Conclusions

In short, new class of biodegradable non-PEGylated polycaprolactone based nanoscaffolds were designed for the delivery of anti-cancer drugs like Doxorubicin. Silyl protected hydroxyl containing caprolactone monomers were successfully designed using multistep reactions, which were polymerized by ROP to synthesize homopolymers and block copolymers, the deprotected homopolymers were completely water soluble, while the block copolymers were dispersible in water, and they self-assembled in water to form spherical micelles, which were capable of loading anti-cancer drugs like doxorubicin in the hydrophobic pocket. Cytotoxicity of the nascent polymers were tested in MCF 7 cell lines and they were non-toxic up to 60 µg/ml. Confocal microscopy images showed the cellular uptake of DOX loaded micelles. Flow cytometric measurements were done to quantify the cellular uptake. Cellular uptake of DOX loaded nanoparticles were 6 folds higher than that of free DOX. Hence a completely biodegradable non-PEGylated polycaprolactone based nanoscaffolds were designed for anti-cancer drug delivery to cancer cells.

5. References

1. Feng, Hongbo; Lu, Xinyi; Wang, Weiyu; Kang, Nam-Goo; Mays, Jimmy. Block copolymers: synthesis, self-assembly and applications. *Polymers.* **2017**, *494*, 500-432.
2. Gaucher, Genevieve; Dufresna, Marie-Helene; Sant, Vinayak; Kang, Ning; Maysinger, Dusica; Leroux, Jean. Block copolymer Micelles: preparation characterization and application in drug delivery. *Journal of controlled release*. **2005**, *109*, 169-188.
3. Li, Chengming; Tang, Yiqing; Armes, Steven. Synthesis and characterization of biocompatible thermo-responsive gelators based on ABA triblock copolymers. *Biomacromolecules* **2005,** *6*, 994-999.
4. Benoit, D.; Harth, E.; Fox, P.; Waymouth, R.M.; Hawker, C.J. Accurate structural control and block formation in the living polymerization of 1, 3-dienes by nitroxide-mediated procedures. *Macromolecules* **2000**, *33*, 363–370.
5. Mai, Yiyong; Eisenberg, Adi. Self assembly of block copolymers. *Chem. Soc. Rev*, **2012**, *41*, 5969-5985.
6. Matsumura, Y; Maeda, H. A new concept for macromolecular therapeutics in cancer chemotherapy: mechanism of tumoritropic accumulation of proteins and the antitumor agent smancs**.** *Cancer Res.* **1986**, *46*, 6387-6392**.**
7. Zhong, Yinan; Meng, Fenghua; Deng, Chao; Zhong, Zhiyuan. Ligand directed active tumor targeting polymeric nanoparticles for cancer chemotherapy. *Biomacromolecules.* **2014**, *15*, 1955-1969.
8. Surnar, Bapurao; Jayakannan, M. Structural engineering of biodegradable PCL block copolymer nanoassemblies for enzyme controlled drug delivery in cancer cells. *ACS biomater. Sci. Eng.* **2016**, *2*, 1926-1941.
9. Kutikov, Artem; Song, Jie. Biodegradable PEG based amphiphilic block copolymers for tissue engineering applications. *ACS biomater. Sci. Eng.* **2015**, *1*, 463-480.
10. Gross, Richard; Kalra, Bhanu. Biodegradable polymers for the enivironment. *Science.* **2002**, *297*, 803-807.
11. Rong, Tong. New chemistry in functional aliphatic polyesters. *Ind. Eng. Chem. Res.* **2017**, *56*, 4207-4219.
12. Nuykan, Oskar; Pask, Stephan. Ring opening polymerization an introductory review. *Polymers* **2013**, *5*, 361-403.
13. Jerome, Christine ; Lecomte, Philippe. Recent advancements in the synthesis of aliphatic polyesters by ring opening polymerization. *Advanced drug delivery review.* **2008**, *60*, 1056-1076.
14. Labet, Marianne; Thielemans, Wim. Synthesis of polycaprolactone: a review. *Chem. Soc. Rev.* **2009**, *38*, 3483-3504.
15. Woodruff, Maria; Hutmacher, Dietmar. The return of a forgotten polymer-Polycaprolactone in the 21st century. *Prog. Polym, Sci.* **2010**, *631*.
16. Hu, Hang; Xiao, Chen; Wu, Honglian; Li, Yihui; Zhou, Qing; Tang, Yuxiang; Yu, Chan; Yang, Xiangliang; Li, Zifu. Nanocolloidosomes with selective drug release for active tumor targeting imaging guided photothermal/chemo combination therapy. *ACS Appl. Mater. Interfaces* **2017**, *9*, 42225-42248.

17. Rainbolt, Elizabet; E, Katherine; Biewer, Michael ; Stefan, Mihaela. Recent developments in micellar drug carriers featuring substituted polycaprolactones. *Polym. Chem.* **2015**, *6*, 2369- 2381.
18. Chen, Tingting; Cai, Tongjiang; Jin, Qiao; Ji, Jian. Design and fabrication of functional polycaprolactone. *E-polymers* **2015**, *15*, 3-13.
19. Wang, Guanjun; Shi, Yan; Fu, Zhifeng; Yang, Wantai; Huang, Qigu; Zhang, Yudong. Controlled synthesis of poly(3-caprolactone)-graft-polystyrene by atom transfer radical polymerization with poly(3-caprolactone-co-a-bromo-3-caprolactone) copolymer as macroinitiator*. Polymer* **2005**, *46*,10601–10606.
20. Liu, Jianjing; Zhang, Yan; Yan, Jinliang; Lang, Meidong. Synthesis and solution properties of pH responsive methoxy poly(ethyleneglycol)-b-poly(g-amino-3-caprolactone). *J. Mater. Chem*. **2011**, *21*, 6677.
21. Surnar, Bapurao; Jayakannan, M. Stimuli responsive polycaprolactone vesicles for dual drug delivery under the gastrointestinal tract. *Biomacromolecules* **2013**, *14*, 4377−4387.
22. Surnar, Bapurao; P.Subash, Pramod; Jayakannan, M. Biodegradable block copolymer scaffolds for loading and deliver cisplatin anti cancer drug. *Z. Anorg. Allg. Chem.* **2014**, *640*, 1119-1126.
23. Surnar, Bapurao; Jayakannan, M. Triple block nanocarrier platform for synergistic cancer therapy of antagonistic drugs. *Biomacromolecules* **2016**, *17***,** 4075−4085.
24. Trollsås, Mikael; Lee, Victor; Mecerreyes, David; wenhielm, Peter; Moller, Michael; Miller, Robert; Hedrick, James. Hydrophilic aliphatic polyesters: design, synthesis and ring opening polymerization of functional cyclic esters. *Macromolecules* **2000,** *33,* 4619-4627.
25. Chang, Longlong; Deng, Liandong; Wang, Weiwei; Lv, Zesheng; Hu, Fuqiang; Dong, Anjie; Zhang, Jianhua. Poly(ethyleneglycol)‑b‑Poly(ε-caprolactone-co-γ-hydroxyl-ε-caprolactone) bearing pendant hydroxyl hroups as nanocarriers for doxorubicin delivery. *Biomacromolecules* **2012**, *13*, 3301−3310.
26. Zhou, Shaobing; Deng, Xianmo; Yang, Hua. Biodegradable poly caprolactone poly(ethylene glycol) block copolymers: characterization and their use as drug carriers for a controlled delivery system. *Biomaterials* **2003**, *24*, 3563**–**3570.
27. Hao, Jing; Servello, John; Sista, Prakash; Biewer, Michael; Stefan, Mihaela. Temperature-sensitive aliphatic polyesters: synthesis and characterization of γ-substituted caprolactone monomers and polymers. *J. Mater. Chem.* **2011**, *21*, 10623-10628.
28. Rainbolt, Elizabeth; Miller, Jason; Washington, Katherine; Senevirathne, Suchithra; Biewer, Michael; Siegwart, Daniel; Stefan, Mihaela. Fine-tuning thermoresponsive functional poly(ε-caprolactone)s to enhance micelle stability and drug loading. *J. Mater. Chem. B***, 2015**, *3*,1779-1787.
29. Malhotra, Mehak; Surnar, Bapurao; Jayakannan, M. Polymer topology driven enzymatic biodegradation in polycaprolactone block and random copolymer architectures for drug delivery to cancer cells. *Macromolecules* **2016**, *49*, 8098−8112.